8-2017

Preferential Flow Systems Amended with Biogeochemical Components: Imaging of a Two-Dimensional Study

Ashley Rose Pales
Clemson University, ashleypales@gmail.com

PREFERENTIAL FLOW SYSTEMS AMENDED WITH BIOGEOCHEMICAL COMPONENTS: IMAGING OF A TWO-DIMENSIONAL STUDY

A Thesis
Presented to
the Graduate School of
Clemson University

In Partial Fulfillment
of the Requirements for the Degree
Master of Science
Hydrogeology

---

by
Ashley Rose Pales
August 2017

Accepted by:
Dr. Christrophe Darnault, Committee Chair
Dr. Brian Powell
Dr. Stephen Moysey
Dr. Lawrence Murdoch

ABSTRACT

The rhizosphere is the region of soil directly impacted by a plants roots, both physically (root growth) and chemically (water and nutrient uptake via organic compounds). The chemical components exuded by a plants roots can be lumped into two categories; mucilage and exudates. Mucilage effects on flow have been widely studied, though the independent effects of exudates have not. The objective of this research is to investigate the effects of plant root exudates on the infiltration processes through a porous media. This is done by (1) characterizing the solid-liquid and liquid-gas interfaces of the exudate solutions used for the flow experiments, and (2) conduct 2-Dimensional light transmission method infiltration flow experiments. For the interfacial characterization citrate generally was the most effective exudate at reducing the contact angle,19% and 29% reduction, and surface tensions, 6.5% and 3% reduction, at both concentrations respectively. In the flow experiments, saturation overshoot was seen in the control, citrate, and tannic acid at both concentrations. Additionally, for the higher concentration exudate solutions greater horizontal saturation dispersion is seen along the edges of the finger pathways, as compared to the low concentration systems. Interfacial characterization of the exudate solutions determined that unnaturally high concentrations of exudates do not have a significant increased effect on the wettability when compared to the effects seen by natural concentrations. Ultimately, the 2- Dimensional light transmission method tank experiments illustrated additional significant differences between the varying exudate solutions through their vertical and horizontal water saturation profiles, then were otherwise unseen through the interfacial characterization.

2- Dimensional light transmission methodologies are a novel tool for visualizing the subsurface flow environment, and allow for insights to be made, that may otherwise remain unseen.

ACKNOWLEDGMENTS

I would like to thank my advisor Dr. Christophe Darnault, and my committee members their support and guidance with this project. I would also like to thank my lab group and all those apart of the DOE EPSCoR Project, without your help and expertise in a multitude of diverse disciplines this work could not be possible. This material is based upon work supported by the U.S. Department of Energy Office of Science, Office of Basic Energy Sciences and Office of Biological and Environmental Research under Award Number DE-SC-00012530.

TABLE OF CONTENTS

Page

LIST OF TABLES

Table Page

LIST OF FIGURES

CHAPTER ONE

INTRODUCTION

1.1. ANDROPOGON VIRGINICUS

The plant species used in this work is *Adropogon Virginicus*, more commonly referred to as broomsedge bluestem (USDA NRCS, 2000). It is a common drought tolerant, C4, perennial grass species that covers roughly 40% of the USA, and is typically found on the edges of forests or in disturbed land areas (USDA NRCS, 2000). It prefers acid to neutral soils (pH4.5-8.0), and can survive in infertile soils with low nitrogen or phosphorus (USDA NRCS, 2000). For this reason, *A. virginicus* is often an indicator plant for infertile soils (USDA NRCS, 2000). The shoots of the plant can grow to a height of two to four feet, and has a shallow rooting system (USDA NRCS, 2000). *A. virginicus* is one of the first species to return to disturbed land sites such as, coalfields, stripe mine sites, or other brownfield locations (Cumming & Ning, 2003; Ning & Cumming, 2001). It has been studied, among other plant species, to understand plant tolerance levels and tolerance mechanisms for contaminants typically associated with mining operations, such as; aluminum, heavy metals, and oxidative stresses (Ezaki et al., 2008; Cumming & Ning, 2003; Ning & Cumming, 2001).

1.2. THE RHIZOSPHERE AND ROOT ZONE

The rhizosphere is the region of soil directly impacted by a plants roots, both physically and chemically (Walker et al., 2003). It is in the rhizosphere where a plants roots grow, exudate organic compounds, and uptake water and nutrients (Cotrufo et al.,

2013). Physical impacts to the soil region include macropore tunnels created by root growth, and compaction and aggregation due to the exuded root compounds impacts (Cotrufo et al., 2013; McCully, 1999; Passioura, 1988). Additionally, the rhizosphere is also impacted by decomposing organic matter, detritus, microorganisms, and fauna; which all play key roles in creating an active and healthy rhizosphere (Cotrufo et al., 2013). Ultimately, understanding the rhizosphere in detail is a difficult feat due to the extreme complexity and compounding effects of variables present in the natural environment, and the necessary over simplification of most laboratory experiments (McCully, 1999).

Current work has focused heavily on the biological aspects of the plant physiology and root growth characterization (McCully, 1999; Passioura, 1988). Understanding transpiration, xylem transport, and root developmental stages, are all very important components of this system. However, understanding the chemical component of these systems is still an area of active research (Walker et al., 2003; Hawes et al., 2000). The chemical components exuded by a plants roots can be lumped into two categories; mucilage and exudates. Mucilage is a viscous excretion that serves a multitude of purposes, such as; lubrication to smooth passages for root growth, slowing root desiccation, and retaining water close to the roots, which is especially useful when water is scarce (Walker et al., 2003; McCully, 1999; Passioura, 1988;). Studies on mucilage have found that it aids in extended water retention, even when the rest of the soil column has dried out (Zarebanadkouki et al., 2016). However, it is not a permanent solution, once the plant has absorbed the stored water, the mucilage become hydrophobic

(Zarebanadkouki et al., 2016). It has been hypothesized that as the water is taken up into the plant the hydrophilic ends of the molecules are attracted to the soil grains, and the thin film of water left behind, leaving the hydrophobic ends facing outward on the soil grains (Zarebanadkouki et al., 2016). Zarebanadkouki et al. (2016) found that after a soil was left to dry out it took multiple rewetting events for the soil to lose its hydrophobic tendencies.

Plant root exudates are specialized organic compounds a plant excretes from its root tips to assist in nutrient uptake; individual exudates are designed to uptake specific nutrients (Read et al., 2003; Walker et al., 2003; McCully, 1999; Passioura, 1988). One mechanism that plant root exudates utilize, is impacting the flow system in the root zone via the solid-liquid and liquid-gas interfaces (Passioura, 1988). The matric potential variations within the root zone are a key component in determining the overall water potential for the plant-soil interactions (Read et al., 2003; Campbell, 1985). Reductions in the contact angle and surface tension of a liquid lead to a reduced amount of suction that a plant needs to potentially exert (Passioura, 1988; Read et al., 2003). This is particularly beneficial when water is scarce; similar to other plant water retention mechanisms, mucilage. In this regard, plant root exudates act similarly to surfactants in increasing the wettability of a fluid in a system (Read et al., 2003; Passioura, 1988). This relationship allows for the comparison of these plant compounds to other well studied surfactants, and the impacts they have on the interfacial characteristics and hydraulic conductivities.

1.3. SURFACTANTS

Surface active agents, surfactants, are used widely in the world for a variety of purposes, such as, hand soap and detergents. They can be ionic, anionic, or nonionic, and their purpose is to reduce the surface tension between a liquid-liquid or liquid-solid interface. While plant exudate effects on wettability and flow are limited, there is an abundance of work that has been done on the effects surfactants have on hydraulic properties. Several works have studied the influence non-ionic surfactants have on unsaturated water flow, viscosity, capillarity, solute transport, hydraulic properties, and soil properties (Karagunduz et al., 2015; Abu-Zreig et al., 2003; Henry and Smith, 2002, 2006; Henry et al., 1999, 2001, 2002). All the studies found that the surfactants, regardless of ionic state, reduced the surface tension of the fluid, though flow characteristics did vary from surfactant to surfactant. Additionally, another generalization was that flow was dominated by the movement from high surfactant concentration to low/no surfactant concentration, which is expected.

Karagunduz et al. (2015) found that the non-ionic surfactant Triton X-100 increased the hydraulic conductivity at the wetting front, but reduced it behind the saturation front. Whereas, Abu-Zreig et al. (2002) looked at two non-ionic surfactants, Rexol and Rexonic, and found that these surfactants did little to impact the hydraulic characteristics of the soil, except for a slight decrease in the hydraulic conductivity. Henry and Smith (2002, 2006), and Henry et al. (1999, 2001, 2002) extensively looked at the influence of a specific non-ionic surfactant, 7% 1-butanol. They found that the 7% 1-butanol reduced the capillarity and air-entry value of the fluid and induced the flow significantly. They assumed that this decrease would lead to thin, long finger formation,

but their modeling found that the width of the finger increased and the fluid gradient extended further than the water only tests. Henry et al. (1999) also compared the non-ionic results to an anionic surfactant, myristyl alcohol, which also reduced the surface tension and capillarity, but the surfactant finger formation was limited to the original flow zones.

Mingorance et al. (2007) studied the effects of all three types of surfactants; Triton X-100 (non-ionic), Aerosol 22 (anionic), and hexadecyl trimethyl ammonium bromide (HDTMA) (cationic). They found for the anionic and cationic surfactants the saturated hydraulic conductivity was reduced, as was the permeability of the soil. Gellner et al. (2006) also studied HDTMA and found that there were no significant changes in the soil hydraulic properties which is different from what Mingorance et al. concluded. A study by Bashir et al. (2011) concluded that the anionic surfactant, DOWFAX 8390, behaved similarly to a fluid with a reduced surface tension of 49mN/m. Abu-Zreig et al. (2003) which found the anionic surfactant Sulphonic significantly impacted the hydraulic properties of the soils, via a decrease in capillary rise and penetrability, as well as, an increase in the contact angle. Pin-Hua et al. (2006) found that an anionic surfactant, sodium dodecylbezenesulfonate (SDBS), behaved differently depending on the concentration of the surfactant and the soil type it was exposed to. Increased concentrations of the SDBS increased the saturated hydraulic conductivity in the Na-soil, whereas the saturated hydraulic conductivity decreased in the Ca-soils. These variations in surfactant effects on flow through soils illustrates the complex interactions of the multitude of available surfactants and various soil types. Simply put these systems, while

well studied, are highly variable and extremely complex, not unlike the interactions experienced in the rhizosphere.

1.4. FINGERING FLOW

Infiltration is the process of water entering into the soil column. It is a complex nonlinear, hysteresis impacted, unsaturated flow regime that is extremely dependent on the soils chemical and physical properties that contribute to the hydraulic properties of the system (Nimmo, 2009). Flow in the vadose zone is driven mainly by gravity, but also by water pressure gradients (Nimmo, 2009). The water pressure gradients can be effected by biological components (i.e. plant roots, microorganisms), and by physical components (i.e. soil particle size) (Passioura, 1988; Nimmo, 2009). Flow in the vadose is unstable and preferentially driven in one of three ways; macropore flow, funneled flow, or fingering flow (Nimmo, 2009). Components of fingering flow, such as, finger velocity, finger width, and fluid saturation gradient within the finger flow have been experimentally and numerically studied in two-dimensions, in water-air, surfactant-air, and surfactant-water-air systems (Glass et al., 1989c; Glass et al., 1989d; Glass and Nicholl, 1996; DiCarlo et al., 2000; Henry et al., 2001, 2002; Henry and Smith, 2006). Fingering flow can be thought of as a density problem, where the less dense fluid (air) is overlain by a denser fluid (infiltrating water). Gravity drives the denser fluid to penetrate into the less dense fluid as ‘spikes’, or fingers of flow, at known intervals. This concept was modeled and displayed by Elder in 1967 as a thermal transient convection problem,

now-a-days we refer to this concept as the Elder Problem, and it underlies many thermal and fluid principles used today.

1.5. IMAGING

Methodologies to characterize a roots architecture has evolved over the years. Soil coring and washing methods are simple and standard, but do not give a wholistic understanding of the entire root (McCully, 1999). Root systems are made up of two large groups of root, long, thick roots, and short, thin roots (McCully, 1999). During the washing procedures, upwards of 50% of these finer roots are washed away and destroyed, leaving an incomplete understanding of a root systems full extent (McCully, 1999). For this reason, in situ observation of roots is widely used to gain a wholistic understanding of the entire roots architecture (McCully, 1999). Rhizotrons, nuclear magnetic resonance, computer aided tomography, and neutron radiography, are examples of imaging tools used to visualize these systems in situ (McCully, 1999). Carminati et al. (2016) conducted a study to look into the biophysical processes affecting plant root water uptake. They concluded that "*despite detailed images of water content…a general understanding of how the rhizosphere affects root water uptake is still lacking*", and that the missing information needed to solve this problem is understanding the gradient of the water potential in the system (Carminati et al., 2016). Carminati et al. (2016) utilized neutron radiography to image the wet/dry cycling of their root systems, which is a detailed imaging method, however, other methodologies provide the key for future works and improvements in this field.

Research with one-dimension (1D), two-dimensional (2D), and three-dimensional (3D), modeling of infiltration processes and fingering flow had progressed widely from the 1960's through to the present (Philips, 1969; Parlange, 1971; Parlange and Hill, 1976; Glass et al., 1989a; Glass et al., 1989b; Glass et al., 1989c; Glass et al., 1989d; Glass et al., 1990; Glass et al., 1991; Glass and Nicholl, 1996). Thus, creating a need for development of experimental apparatuses to confirm the mathematical modeling. This need for an inexpensive, nondestructive, quick response methodology lead to the development of the light transmission method (LTM) by N.T. Hoa in 1981. Neutron radiography imaging was the standard methodology, but Hoa (1981) recognized the need for a simple and inexpensive methodology. He found that the ability for a lights intensity to penetrate an opaque media, quartz sand, increased as the number of pores in the system became saturated; and decreased as those pores became air filled again (Hoa, 1981). Simply put, water filled pores favored the transmission of light through the porous media (Hoa, 1981). The only drawback of this method, was that a calibration was required for each system (Hoa, 1981). This original concept remains largely unchanged, though the experimental systems and analysis have been in constant flux since the creation of this methodology. Flow chambers, flow slabs, 2D slabs, rhizotrons, and 2D tanks, are all of the names employed by various works, who study thin sections of porous media and their associated flow systems. The work presented here is a rough extension on the works by Darnault et al. (1998, 2001) who used LTM to view fingering flow in water-oil and water-oil-air systems. 2D tanks were developed for this work to visualize infiltration processes and fingering flow phenomena in a porous media.

1.6. PURPOSE AND ORGANIZATION

The objective of this research is to investigate the effects of plant root exudates on the infiltration processes through a porous media. This overarching objective will be fulfilled through an integrative research approach:

1. Create a functional and flexible experimental set up able to work with the light transmission method, gamma scanning apparatuses, and geochemical foil analysis, to produce high spatial and temporal data resolution.
2. Characterize the processes of the solid-liquid and liquid-gas interfaces of various biochemical compound solutions (citrate, oxalate, tannic acid, and SRNOM) at a range of concentrations from naturally occurring to unnaturally elevated (0.1-500 mg/L).
3. Conduct 2D tank experiments with light transmission methodologies, to visualize and characterize infiltration processes, in order to quantify the effects of different exudate solution chemistry.

This thesis is organized into three chapters including the Introduction (Chapter 1) and Conclusions (Chapter 3). The body chapter (Chapter 2) is written and structured as an independent manuscript intended for publication.

REFERENCES

Abu-Zreig, M., Rudra, R. P., & Dickinson, W. T. (2003). Effect of application of surfactants on hydraulic properties of soils. *Biosystems Engineering*, *84*(3), 363-372. doi:10.1016/S1537-5110(02)00244-1

Bashir, R., Smith, J. E., & Stolle, D. E. (2011). The effect of ionic strength on surfactant-induced unsaturated flow. *Canadian Geotechnical Journal*, *48*(4), 644-654. doi:10.1139/T10-096

Campbell, G.S. (1985). Soil physics with basic transport models for soil-plant systems. Amsterdam, The Netherlands: Elsevier.

Carminati, A., Zarebanadkouki, M., Kroener, E., Ahmed, M. A., & Holz, M. (2016). Biophysical rhizosphere processes affecting root water uptake. Annals of Botany, 118, 561-571. doi: 10.1093/aob/mcw113

Cotrufo, M.F., Wallenstein, M.D., Boot, C.M., Denef, K., & Paul, E. (2013). The Microbial Efficiency-Matrix Stabilization (MEMS) framework integrates plant litter decomposition with soil organic matter stabilization: do labile plant inputs form stable soil organic matter?. Global Change Biology, 19, 988-995. Doi:10.1111/gcb.12113

Cumming JR, Ning J (2003) Arbuscular mycorrhizal fungi enhance aluminium resistance of broomsedge (Andropogon virginicus L.). Journal of Experimental Botany 54:1447-1459

Darnault, C. J. G., Throop, J. A., DiCarlo, D. A., Rimmer, A., Steenhuis, T. S., & Parlange, J. Y. (1998). Visualization by light transmission of oil and water

contents in transient two-phase flow fields. *Journal of Contaminant Hydrology, 31*(3-4), 337-348. doi:10.1016/S0169-7722(97)00068-5

Darnault, C. J. G., DiCarlo, D. A., Bauters, T. W. J., Jacobson, A. R., Throop, J. A., Montemagno, C. D., & Steenhuis, T. S. (2001). Measurement of fluid contents by light transmission in transient three-phase oil-water-air systems in sand. *Water Resources Research, 37*(7), 1859-1868. doi:10.1029/2000WR900380

DiCarlo, D., Bauters, T., Darnault, C., Wong, E., Bierck, B., Steenhuis, T., & Parlange, J. (2000). Surfactant-induced changes in gravity fingering of water through a light oil. *Journal of Contaminant Hydrology, 41*(3-4), 317-334. doi:10.1016/S0169-7722(99)00078-9

Ezaki, B., Nagao, E., Yamamoto, Y., Nakashima, S., & Enomoto, T. (2008). Wild plants, Andropogon Virginicus L. and Miscanthis sinensis Ander, are tolerant to multiple stresses including aluminum, heavy metals, and oxidative stresses. Plant Cell Reports, 27(5), 951-961. DOI: 10.1007/s00299-007-0503-8

Gellner, W. J.,II, Zhao, X., Girand, M., Boyd, S. A., & Voice, T. C. (2006). Hydraulic conductivity of soil sorptive zones created by in situ injection of a cationic surfactant. *Journal of Environmental Engineering-Asce, 132*(12), 1659-1663. doi:10.1061/(ASCE)0733-9372(2006)132:12(1659)

Glass, R., & Nicholl, M. (1996). Physics of gravity fingering of immiscible fluids within porous media: An overview of current understanding and selected complicating factors. *Geoderma, 70*(2-4), 133-163. doi:10.1016/0016-7061(95)00078-X

Glass, R., Cann, S., King, J., Baily, N., Parlange, J., & Steenhuis, T. (1990). Wetting front instability in unsaturated porous-media - a 3-dimensional study in initially dry sand. *Transport in Porous Media, 5*(3), 247-268. doi:10.1007/BF00140015

Glass, R., Oosting, G., & Steenhuis, T. (1989a). Preferential solute transport in layered homogeneous sands as a consequence of wetting front instability. *Journal of Hydrology, 110*(1-2), 87-105. doi:10.1016/0022-1694(89)90238-2

Glass, R., Parlange, J., & Steenhuis, T. (1989b). Wetting front instability .1. theoretical discussion and dimensional analysis. *Water Resources Research, 25*(6), 1187-1194. doi:10.1029/WR025i006p01187

Glass, R., Parlange, J., & Steenhuis, T. (1991). Immiscible displacement in porous-media - stability analysis of 3-dimensional, axisymmetrical disturbances with application to gravity-driven wetting front instability. *Water Resources Research, 27*(8), 1947-1956. doi:10.1029/91WR00836

Glass, R., Steenhuis, T., & Parlange, J. (1989c). Wetting front instability .2. experimental-determination of relationships between system parameters and two-dimensional unstable flow field behavior in initially dry porous-media. *Water Resources Research, 25*(6), 1195-1207. doi:10.1029/WR025i006p01195

Glass, R., Steenhuis, T., & Parlange, J. (1989d). Mechanism for finger persistence in homogeneous, unsaturated, porous-media - theory and verification. *Soil Science, 148*(1), 60-70. doi:10.1097/00010694-198907000-00007

Hawes, M.C., Gunawardena, U., Miyasaka, S., & Zhou, X. (2000). The role of root boarder cells in plant defense. Trends in Plant Science, 5(3), 128-133. Doi: 10.1016/S1360-1385(00)01556-9

Henry, E. J., & Smith, J. E. (2002). The effect of surface-active solutes on water flow and contaminant transport in variably saturated porous media with capillary fringe effects. *Journal of Contaminant Hydrology, 56*(3-4), 247-270. doi:10.1016/S0169-7722(01)00206-6

Henry, E. J., & Smith, J. E. (2006). Numerical demonstration of surfactant concentration-dependent capillarity and viscosity effects on infiltration from a constant flux line source. *Journal of Hydrology, 329*(1-2), 63-74. doi:10.1016/j.jhydrol.2006.02.008

Henry, E. J., Smith, J. E., & Warrick, A. W. (1999). Solubility effects on surfactant-induced unsaturated flow through porous media. *Journal of Hydrology, 223*(3-4), 164-174. doi:10.1016/S0022-1694(99)00116-X

Henry, E. J., Smith, J. E., & Warrick, A. W. (2001). Surfactant effects on unsaturated flow in porous media with hysteresis: Horizontal column experiments and numerical modeling. *Journal of Hydrology, 245*(1-4), 73-88. doi:10.1016/S0022-1694(01)00338-9

Henry, E. J., Smith, J. E., & Warrick, A. W. (2002). Two-dimensional modeling of flow and transport in the vadose zone with surfactant-induced flow. *Water Resources Research, 38*(11), 1251. doi:10.1029/2001WR000674

Hoa, N. (1981). A new method allowing the measurement of rapid variations of the water-content in sandy porous-media. *Water Resources Research, 17*(1), 41-48. doi:10.1029/WR017i001p00041

Karagunduz, A., Young, M. H., & Pennell, K. D. (2015). Influence of surfactants on unsaturated water flow and solute transport. *Water Resources Research,* 51(4), 1977-1988. doi:10.1002/2014WR015845

McCully, M. E. (1999). Roots in soil: Unearthing the complexities of roots and their rhizospheres. *Annu. Rev. Plant Physiol. Plant Mol. Biol*., 50, 695-718.

Mingorance, M. D., Fernandez Galvez, J., Pena, A., & Barahona, E. (2007). Laboratory methodology to approach soil water transport in the presence of surfactants. *Colloids and Surfaces A-Physicochemical and Engineering Aspects, 306*(1-3), 75-82. doi:10.1016/j.colsurfa.2007.04.026

Nimmo, J.R. (2009). Vadose Water. *Encyclopedia of inland waters*, 1, 766-777.

Ning J, Cumming JR. (2001). Arbuscular mycorrhizal fungi alter phosphorus relations of broomsedge (Andropogon virginMcCully, M. E. (1999). Roots in soil: Unearthing the complexities of roots and their rhizospheres. Annual Review Plant Physiology Plant Molecular Biology, 50, 695-718.

Parlange, J. (1971). Theory of water-movement in soils .1. one-dimensional absorption. *Soil Science, 111*(2), 134-&. doi:10.1097/00010694-197102000-00010

Parlange, J., & Hill, D. (1976). Theoretical-analysis of wetting front instability in soils. *Soil Science, 122*(4), 236-239. doi:10.1097/00010694-197610000-00008

Philip, J. R. (1969). Advances in hydroscience. Book, pg 215-296.

Passioura, J.B. (1988). Water transport in and to roots. Annu. Rev. Plant Physiol. Plant Mol. Biol., 39, 245-265.

Rao Pin-Hua, He Ming, Yang Xian, Zhang You-Chi, Sun Shou-Qin, & Wang Jiang-Sheng. (2006). Effect of an anionic surfactant on hydraulic conductivities of sodium- and calcium-saturated soils. *Pedosphere, 16*(5), 673-680. doi:10.1016 /S1002-0160(06)60102-1

Read, D. B., Bengough, A. G., Gregory, P. J., Crawford, J. W., Robinson, D., Scrimgeour, C. M., Young, I.M., Zhang, K., & Zhang, X. (2003). Plant roots release phospholipid surfactants that modify the physical and chemical properties of soil. New Phytologist, 157(2), 315-326. doi:10.1046/j.1469-8137.2003.00665.

USDA Natural Resources Conservation Service. (2000). The PLANTS database. <https://plants.usda.gov/core/profile?symbol=ANVI2>. 001106. National Plant Data Center, Baton Rouge, LA. Accessed on 1/31/2017.

USDA Natural Resources Conservation Service. (2000). Plant Guide; Broomsedge Bluestem. <https://plants.usda.gov/plantguide/pdf/pg_anvi2.pdf>. National Plant Data Center, Baton Rouge, LA. Accessed on 1/31/2017.

Walker, T.S., Bais, H.P., Grotewold, E., & Vivanco,J.M. (2003). Root exudation and rhizosphere biology. Plant Physiology, 132, 44-51. Doi:10.1104/pp.102.019661.

Zarebanadkouki, M., Carminati, A., & Ahmed, M. A. (2016). Hydrualic conductivity of the root-soil interface of lupin in sandy soil after drying and rewetting. Plant Soil, 398, 267-280. Doi:10.1007/s11104-015-2668-1.

CHAPTER TWO

PREFERENTIAL FLOW SYSTEMS AMENDED WITH BIOGEOCHEMICAL COMPONENTS: IMAGING OF A TWO-DIMENSIONAL STUDY

Ashley Pales, Biting Li, Heather Clifford, Shyla Kupis, Nimisha Edayilam, Dawn Montgomery, Wei-zhen Liang, Mine Dogan, Nishanth Tharayil, Nicole Martinez, Stephen Moysey, Brian Powell, and Christophe J. G. Darnault

Keywords: Infiltration; Wetting front instability; Fingered flow; Plant exudates; Interface phenomena; Light transmission method

ABSTRACT

The vadose zone is a highly interactive heterogeneous system through which water enters into the subsurface system by infiltration. This paper details the effects of simulated plant exudate solutions upon unstable flow patterns in a porous media (ASTM silica sand; US Silica, Ottawa, IL, USA) through the use of two-dimensional (2D) tank light transmission method (LTM). The contact angle and surface tension of the four simulated plant exudate solutions (i.e. oxalate, citrate, tannic acid, and Suwannee River Natural Organic Matter) were analyzed to determine the liquid-air and liquid-solid interface characteristics of each. To determine if the unstable flow formations were dependent on the type and concentration of the simulated plant exudates, the analysis of the effects of the simulated plant exudate solutions were compared to a control rainwater solution. The differences in the fingering flow were quantified with the finger geometries; the velocity of finger propagation, the vertical and horizontal water saturation profiles, and the saturation overshoot at the fingertips. Significant differences in the interface processes indicated a decrease between the control and the exudate solutions tested; specifically, the control at 64.5 θ and 75.75 Nm/m, to the low concentration of citrate at 52.6 θ and 70.8 Nm/m. The changes in finger geometries and velocity of propagation between the control solution and the simulated plant exudate solutions further demonstrates that the plant exudates increased the wettability and mobility of the solutions during the infiltration process in unsaturated porous media.

2.1. INTRODUCTION

Infiltration of water in soil is a fundamental element of the hydrologic cycle (Horton, 1933). The infiltration process controls the existence of water and life at the soil-atmosphere interface, and is especially important to soil moisture (Rodriguez-Iturbe et al., 1999) and vegetation (Liang et al., 1994). Consequently, the knowledge of water flow and contaminant transport through soils is critical for the management and development of groundwater resources. Understanding the movement of water in soils is particularly valuable in terms of groundwater recharge and contaminant loading. The infiltration process is impacted by the physico-chemical properties and biological activities that occur in the unsaturated zone of the soil (vadose zone), as well as the human activities and the climate (Glass et al., 1991).

In general, water flow and contaminants transport in soil are heterogeneous (Bien et al., 2013; Dorr and Munnich, 1991; Klos et al., 1999; McBride, 1998; Muller and Prohl, 1993; Wang et al., 2006). These heterogeneities occur in the form of spatial and temporal variability in soil hydraulic properties, water supply rate and contaminant amount, affect the hydrologic response to precipitation, and therefore influence the quantity and quality of both groundwater and surface water resources (Beven and Germann, 2013; Clothier et al., 2008; Jarvis et al., 2016; Jarvis, 2007; Weiler, 2017). Preferential flow, which is one such heterogeneity, is rather the rule than the exception in hydrologic and earth sciences (Bundt et al., 2000; Smith and Elder, 1999). Preferential flow in soil is defined as the concentration of flow of water into a small fraction of the volume of the porous media, which increases the flow velocity, bypasses most of the soil

matrix (Hendrickx and Flury, 2001), and thus reduces the time needed for the attenuation of contaminants, and transport of contaminants to aquifers. Preferential flow, has been the subject of numerous studies (e.g. (Allaire et al., 2009; Andreini and Steenhuis, 1990; Clothier et al., 2008; Flury et al., 1994; Gerke et al., 2010; Glass et al., 1989d; Kung, 1990a; Ritsema et al., 1993; Simunek et al., 2003)). Preferential flow in the soil may occur through several mechanisms, such as macropore flow (e.g., connected and disconnected macropores, cracks, earthworm burrow, root channels) (Beven and Germann, 2013; Bouma and Dekker, 1978), fingered flow (i.e., wetting front/gravity-driven instability or "fingers") (Glass et al., 1989c, 1989d; Wang et al., 2003a), and funnel flow (e.g., layering or textural interfaces) (Kung, 1990a, 1990b). Preferential flow serves as the catalyst for the rapid transport of solutes and particles, including contaminants such as pesticides, nutrients, metals, pathogens, radionuclides, antimicrobials, and nonaqueous phase liquids (NAPLs) with little interaction into the soil matrix, which can significant degrade groundwater quality (Boyer et al., 2009; Darnault et al., 2003, 2004; DiCarlo et al., 2000; Engelhardt et al., 2015; Jarvis et al., 2016; Kay et al., 2004, 2005; Kim et al., 2005; Nimmo, 2012; Uyusur et al., 2010, 2015; Zhang et al., 2016).

The stability of an interface between two immiscible fluids in a porous medium has been the subject of numerous research since the 1950's until now, especially in the field of petroleum engineering and in hydrologic sciences (Chouke et al., 1959; Homsy, 1987; van Meurs, 1957; Saffman, 1986; Saffman and Taylor, 1958; Stokes et al., 1986; Tanveer, 1987a, 1987b). When a wetting fluid comes in contact with a dry porous

medium, flow in the porous medium is caused by capillarity, and these capillary forces transfer water in any direction. The development of this flow without the influence of gravity is known as a "sorption" process, and the development without this influence is known as an "infiltration" process (Assouline, 2013). Infiltration process in soil is the particular instance of the dynamics of fluid interfaces and flow in porous media, where infiltration is a downward movement of water into dry unsaturated soils and causes the formation of a gas-water interface, known as the "wetting front". This wetting front propagation can be classified as stable or unstable depending on the non-linearity behavior of the relationship between the soil hydraulic properties and the soil moisture content (Cueto-Felgueroso et al., 2009; Cueto-Felgueroso and Juanes, 2008, 2009a, 2009b; Egorov et al., 2003; Wallach et al., 2013). During a stable infiltration process into a homogeneous porous media and under steady state flux conditions at the surface, a stable wetting front moves downward. While in an unstable infiltration process into a homogeneous porous media and under steady state flow, an unstable wetting front is driven by gravity and stabilized by surface tension resulting from capillary forces present in the porous media, and preferential flow paths ("fingers") are generated (Glass et al., 1989a, 1989b, 1989c; Hill and Parlange, 1972; Kapoor, 1996; Peck, 1965; Selker et al., 1992a; Yao and Hendrickx, 1996). Once these fingered flow phenomena are generated, the flow area is decreased compared with that of the wetting front, and the flux velocities of the fingers increase tremendously (Wallach et al., 2013). Peck (1965) was the first to describe the formation of "tongues" of infiltrating water in sand columns and the entrapment of air below the wetting front. Hill and Parlange (1972) conducted the first

systematic experiment to investigate the phenomenon of wetting front instability. The role and importance of fingered flow in contaminants transport was demonstrated with several cases of groundwater contamination (e.g. (Hillel, 1987; Steenhuis et al., 1990)).

The non-linearity of the governing equations for unsaturated flow through porous media makes a theoretical analysis of water movement in soils and wetting front instability in soils most challenging (Buckingham, 1907; Richards, 1931). Infiltration theories and the development of mathematical solutions to solve the problem of flow in porous media have been the subject of much research, most particularly as evidenced through the seminal work of Jean-Yves Parlange (Parlange, 1971a, 1971b, 1971c, 1972a, 1972b, 1972c, 1972d, 1972e, 1973, 1975; Parlange and Aylor, 1972). Analytical and quasi-analytical solutions of the flow equation have been developed through the time expansion (Philip, 1969, 1975) and integral approaches (Parlange, 1971b, 1972e). Further Saffman and Taylor (1958) and Chouke et al., (1959) concluded that the development of wetting front instability resulted from unsaturated flow (Pendexter and Furbish, 1991; Raats, 1973; Selker et al., 1992c), an increase in hydraulic conductivity with depth (Hill and Parlange, 1972; van Ommen et al., 1989), a decrease in soil wettability with depth (Hill and Parlange, 1972; Hillel, 1987; Philip, 1975; Raats, 1973; Tamai et al., 1987), water repellency (Dekker and Ritsema, 1994; Ritsema et al., 1993; Ritsema and Dekker, 1994), a redistribution of infiltration after the end of rainfall or irrigation (Philip, 1975), and air entrapment (Peck, 1965; Philip, 1975; Raats, 1973; Wang et al., 1998).

In addition to these theoretical analyses, numerous experimental studies have been undertaken to elucidate the instability of the wetting front propagation, specifically

in layered soils (Hill and Parlange, 1972), under increased air pressure ahead of the wetting front and soil heterogeneity (White et al., 1976, 1977), and in layered soils with variable initial soil moisture (Diment and Watson, 1985). These conditions are prevalent in soils through the world. The instability of wetting front has been studied primarily in two-dimensional tanks entailing the generation of a two-dimensional fingered flow (e.g. (Baker and Hillel, 1991; Bauters et al., 2000a; DiCarlo, 2004; Glass et al., 1989a, 1989c, 1989d, Selker et al., 1992a, 1992b, 1992c)). Laboratory experiments designed to examine the infiltration process in homogeneous porous media have confirmed the constantly formation of fingered flow (Bauters et al., 2000b; Diment and Watson, 1985; Glass et al., 1989d; Lu et al., 1994; Selker et al., 1992a; Sililo and Tellam, 2000; Wang et al., 2003b, 2004; Yao and Hendrickx, 2001). Also experimental observations have demonstrated that the fingers that develop the most rapidly will convey most of the flow, while the other initial fingers will be quenched (Glass et al., 1989d; Selker et al., 1992b). The fully formed fingers generated by gravity-driven flow behave like traveling waves (i.e. constant shape and velocity) and the water saturation profile of the fully form fingers exhibit the following pattern: a region of high water saturation directly behind the wetting front, known as the fingertip, i.e. an overshoot at the fingertips; followed by another region of drying where the water content in the finger decrease to a lower and uniform water saturation, known as the finger tail (DiCarlo, 2004; Glass et al., 1989a; Liu et al., 1994; Selker et al., 1992b). Further details on theoretical and experimental research on wetting front instability can be found in extensive reviews (Assouline, 2013; Glass and Nicholl, 1996; De Rooij, 2000; Xiong, 2014).

The vadose zone is a highly interactive heterogeneous system between water, air, soil constituents, flora, and fauna (Bengough, 2012; Hallett et al., 2013; Lehmann et al., 2012) . The rhizosphere is an important component of the vadose zone and is specifically defined as the narrow region of soil that is directly influenced by plant roots themselves and by the root secretions (Hinsinger et al., 2009; McCully, 1999; Passioura, 1988; Read et al., 2003). It has been estimated that about 40% of the precipitation on earth transitions through the rhizosphere (Bengough, 2012). The rhizosphere has a deep effect on the hydrologic processes (Benard et al., 2016), and its interactions in the soil system not only involve the physical effects stemming from soil and root dynamics, but also include biochemical effects from the compounds the roots of a plant can exude from their root tips (Benard et al., 2016; Gregory, 2006; Hinsinger et al., 2009).

There are two main biochemical compounds produced by the plant roots: mucilage and exudates. Mucilage is a viscous substance composed mainly of polysaccharides and some phospholipids (Guinel and McCully, 1986; McCully and Boyer, 1997; Read et al., 2003) the purpose of which is to keep the soil around the roots moist by swelling and adsorbing water (Guinel and McCully, 1986), as well as to control the water repellency of the rhizosphere (Carminati, 2012; Carminati et al., 2010; Moradi et al., 2012). Root exudates comprise mostly sugar, amino acids, and organic acids, and are exuded primarily from the root tips (Carvalhais et al., 2011; McCully, 1999; Passioura, 1988; Read et al., 2003). These exudates play a key role in keeping the contact between the roots and soil particles (Walker et al., 2003), the modulation and mobilization the nutrients (Cakmak et al., 1998; Carvalhais et al., 2011; Wang et al.,

2008), and the maintenance of the rhizosphere hydraulic properties (Ahmed et al., 2014) by providing a large water-holding capacity (McCully and Boyer, 1997), enhancing the movement of water in dry soil, and enabling the roots to get water from dry soils (Ahmed et al., 2014). Individual exudates have specific nutrients (i.e. phosphate, nitrate, potassium) that they are designed to extract from the soil. This unique chemistry thus increases the solubility of the sought-after nutrients to ease the uptake by the plant. In this regard, the exudates act as surfactants within the subsurface by lowering the surface tension and contact angles of the soil pore water, enhancing the wettability, and reducing the suction and energy needed for the plant to extract what is needed (McCully, 1999; Passioura, 1988; Read et al., 2003).

The plant root growth in soil is constrained, however. As water, air, and nutrients resources are scarce, and spatially and temporally heterogeneously available in soil (Hinsinger et al., 2009), plants have evolved various adaptive strategies to adapt to the environment they encounter to their advantage and access these resources. Hydromechanic analyses of soil and water interactions in the rhizosphere have demonstrated that rhizodeposits (i.e. mucilages and exudates) induce water potential gradients near the roots and therefore increase soil moisture near them (Carminati et al., 2010; Gardner, 1960; Ghezzehei and Albalasmeh, 2015; Moradi et al., 2011; Young, 1995) As the water potential decreases near the root to produce a concurrent decrease in soil water content, water moves from the bulk soil to the root surfaces. Although the effect of root exudates on the soil structure and aggregation has been well established (Alami et al., 2000; Czarnes et al., 2000; Ghezzehei and Albalasmeh, 2015; Kaci et al.,

2005; McCully, 1999; Watt et al., 1994), research on the effect of the rhizodeposits (i.e. mucilages and exudates) on soil-water relationship and water dynamics in the rhizosphere is very limited. This is a crucial knowledge gap in terms of the biogeochemical influences on the hydrologic processes occurring in the rhizosphere as stated by Bengough (2012), particularly the effect that root exudates have on the nonequilibrium dynamics of interfaces and flow in porous media. Carminati et al. (2016) recently analyzed the rhizosphere processes to more thoroughly elucidate the system, with a particular focus on determining the role of mucilage in root water uptake. They were particularly interested in determining the biological impacts of wet versus dry mucilage to the system, and how those changes in turn, affected the plants overall ability to uptake water (Carminati et al., 2016). They found that wet mucilage enhances fluid transport, but when dry causes hydrophobic tendencies in the rhizosphere (Carminati et al., 2016). From this analysis they determined a need for new technology and sensor applications to gain a full and detailed understanding of the rhizosphere, regardless of the new methodologies in development for imaging these systems and understanding the plants themselves. Ultimately an enhanced focus in current research to better elucidate the interactions between the biological, chemical, and physical processes that control the rhizosphere is needed. A knowledge of the mechanisms and parameters that govern the wetting front dynamics is most necessary for predicting wetting-front propagation through soil, which in turn makes it possible to predict both soil and groundwater pollution. The non-uniform nature of transport occurring through unstable flow fields means that the transport of contaminants in the subsurface and contaminant loading of aquifer differs from an

assumed one-dimensional modality of movement (Glass et al., 1989b, 1991). Any contamination to the vadose zone contamination means a threat to groundwater, which also means that any remediation undertaken to remove that threat is most challenging (Dresel et al., 2011; Triplett et al., 2011; Wellman et al., 2011).

Indeed, the groundwater at the decommissioned nuclear production Hanford facility in Richland, WA is contaminated with uranium (Qafoku et al., 2004; Rod et al., 2010; Um et al., 2009, 2010) caused from discharge from leaky underground storage tanks of more than 7 tons of uranium through the vadose zone in an alkaline milieu (Jones et al., 2001). This leakage, which occurred from the late 1950s through the 1960s resulted in groundwater contamination in parts of the 300 Area Hanford Site that surpasses the 30 ugL-1 uranium drinking water standard (Waichler and Yabusaki, 2005). Another example of such worrisome contamination is the Nevada Test Site (NTS) in which large quantities of uranium were in the vadose zone, from the approximately 600 underground conducted during its operation (Tompson et al., 2006)

Therefore, the intent of the research described here was to investigate the effects of biochemical compounds from root plants and soil constituents on the spatial and temporal infiltration process, particularly the wetting front stability and fingered flow in a soil-water-air system. The dynamics of interfaces in porous media—gas-water and soil-water interfaces—under the impact of various biochemical compounds were monitored through interfacial tension and contact angle measurements. Utilizing the imaging technique of the light transmission method (LTM) that allows the visualization of fluids content and flow in porous media with high spatial and temporal resolution (Darnault et

al., 1998, 2001; Niemet and Selker, 2001; Weisbrod et al., 2003), we studied the effects of several isolated organic compounds, typically found in the rhizosphere, that were dispersed as artificial rainfall and infiltrate under unsaturated conditions through a homogenous sandy porous media on the wetting front stability and fingered flow phenomena in two-dimensional tank. Ultimately, our understanding of the influence of these isolated exudates upon these infiltration processes and water saturation distribution within the porous media is a significant step forward to fully elucidate the range of interactions controlling flow within the rhizosphere.

2.2. MATERIALS AND METHODS

2.2.1. Simulated Constituent Solution Preparation

In order to reduce the number of active variables present in this work, solutions of simulated plant exudates and soil components were used rather than living plants and soil. A Hoagland Nutrient Solution (HNS) with 0.01 M NaCl (NaCl+HNS) was used as a control to simulate the requisite nutrients required of a plant to survive in a hydroponics system. The HNS was created by combining the components listed in Table 2.1. with 970 mL of ultrapure deionized (DI) water (18.2 MΩ•cm, Millipore Corporation, Billerica, MA) with NaCl (Lot #: 2954C512, VWR Analytical BDH®, Radnor, PA) subsequently added to bring the solution to 0.01 M NaCl. These steps are based on the method developed by Arnon and Hoagland in 1940. Two plant exudates, sodium citrate (S1804-500G, Sigma-Aldrich, Lake Cormorant, MS), and sodium oxalate (Lot #: P17A014, Alfa Aesar, Ward Hill, MA); and two soil components, Suwanee River Natural Organic

Matter (SRNOM, RO isolate, 2R101N, International Humic Substances Society, St. Paul, MN), and tannic acid (Lot #: MKBV0516V, Sigma-Aldrich, Lake Cormorant, MS), were used to create the solutions tested in this work. Using NaCl+HNS as a base solution, different concentrations of the constituents were created to simulate a range of potential concentrations, a list of which is provided in Table 2.2. These concentrations were categorized based on amounts naturally found in the environment (Jones, 1998; Strobel, 2001; Wagoner et al., 1997).

2.2.2. Solution Characterization

A Kruss Easy Drop (FM40Mk2, Kruss GmbH, Germany) was used to obtain the contact angle and surface tension with 5 µL of the various experimental solutions deposited on a 24×60 mm micro cover glass (CAT No. 4404-454, VWR, Radnor, PA) for the contact angle analysis. The Drop Shape Analysis software (Kruss GmbH, Germany) was used with the following settings: contact angle profile defined with circle fitting, drop type – sessile drop, sub-type normal. Images and data were collected every 30 seconds for 3 minutes for both the contact angle and surface tension data. The Kruss Easy Drop DSA1 internally computes the contact angle of a drop using the Young equation (Young, 1805):

$$\sigma_s = \gamma_{sl} + \sigma_l * \cos(\theta) \quad (1)$$

where σ_s is the solid surface tension, σ_l is the liquid surface tension, γ_{sl} is the interfacial tension between the phases, and θ is the contact angle. It also calculates the surface

tension of pendent drops using the Young-Laplace equation (Laplace, 1806; Young, 1805):

$$\Delta P = \sigma * \left(\frac{1}{r_1} + \frac{1}{r_2} \right) \quad (2)$$

where ΔP is the difference in pressure of the inside and outside of the droplet, r_1 and r_2 are the principle radii of the droplet, and σ is the surface tension. By using the characteristic shape and size of the droplets, the equipment can determine the surface tension of the droplet. These variables on a stable solution droplet collected at 90 s are illustrated in Figure 2.1. with all solutions tested in triplicate with the averages, and their associated standard deviations presented in this work (Table 2.3.). A statistical analysis was done for the contact angle and surface tension measurements utilizing a t-test. The surface tension measurements were obtained by suspending the solution as a drop in an open-air environment from a 2 mm diameter needle point. The software was configured with the following settings: drop information – with a needle diameter of 2 mm, a tip level (pixels) of 80, an assumed liquid drop density phase of (g/cm^3) - 0.9975, an embedding phase of 0.0012, a magnification factor (pixels/mm) of 79.827, and an aspect ratio of 1.

2.2.3. Light Transmission Method

Developed by N.T. Hoa, the Light Transmission Imaging Method (LTM) was first used as a rapid, inexpensive method for the visualization of flow in 2D systems (Hoa, 1981), and has since been expanded for use in water-air, oil-water, and water-oil-air systems. The methods used in this work adhere to the methods developed by Darnault et

al. (2001, 1998). The LTM works through the illumination of a thin section of porous media (i.e. 1 inch thick section of silica sand) from behind with a light source. A standard camera is then used to capture the amount of light that transmits through the 2D area for any given condition (unsaturated – fully saturated). These images are recorded in standard RGB (red-green-blue) format, and converted into HSI (hue-saturation-intensity) format. The colors of an image or photograph can be broken down into three distinct layers of the image itself, this is the hue, saturation, and intensity. The hue is the wavelength of the light energy, the saturation is the bandwidth of the wavelength, and the intensity is the total energy value or the amplitude. Upon conversion into this format, information on the water content is discernable. Specific combinations of the HSI format can be used to determine the water content depending on the nature of the 2D system and fluids. Similarly, the porous media is calibrated via saturation to a known percentage and a discrete value is obtained via the HSI format. The experimental design reduced the efficacy of hue and saturation as opposed to intensity; here intensity was used to create the calibration equation for the experiments.

An empirical calibration curve was created using small calibration tanks filled with the silica sand to multiple known water saturation percentage points. The water saturation points were found for 0%, 5%, 10%, 20%, 40%, 60%, 80%, and 100%. The calibration was completed in triplicate to account for potential variations in packing and ambient light pollution. A linear calibration relationship is seen between the water saturation points increasing, and the transmitted intensity increasing, see Figure 2.2. It is important to note that the 80% intensity values read high due to the water drainage, and

thus saturation, of the water in the lower half of the calibration tank. This linear relationship and slope equation were used to convert the intensity values into water saturation values with the Matlab software. Additionally, for each flow experiment, the 0% and 100% intensity values were found and the slope from each experiment was compared to the calibration curve to ensure that the calibrations between experiments were similar.

The 2D tank was constructed using clear 1.3 cm thick polycarbonate plates (8707K153, McMaster-Car, Douglasville, GA) for purposes of visualizing the flow process (Figure 2.3.). The 30.5 × 1.3 × 30.5 cm tank contains four porous plates (0660X01-B01M3, Soilmoisture Equipment Corp., Goleta, CA) along the sloped bottom of the tank, and an effluent port at the base of the slope. For experiments, the tank is fitted to an aluminum stand with an LED light source mounted on the back (36W dimmable, natural white 61 × 61 cm, LPWD-NW6060-36, superbrightleds.com, St. Louis, MO) and rainfall simulator (screw actuator) mounted on top. To prevent reflective and refractive light from affecting the images collected, the excess light from the LED light was blocked to ensure the transmission of only visible light through the tank.

2.2.4. 2D Tank Flow Experimental Design

The 2D tank was secured to the stand prior to packing to minimize jostling and to reduce sand movement, thus decreasing the likelihood of heterogeneity. A packing device was then affixed to the top of the tank and filled with two tank volumes of graded sand that conform to ASTM (American Society for Testing and Materials) C778 standards (US

Silica, Ottawa, IL). The second tank volume of sand allows for the homogeneous packing of the tank to a uniform bulk density of 1.5043 g/cm^3. The US Silica product data sheet described the size of the ATSM graded sand using standard USA STD sieve mesh sizes from 16 – Pan (US Silica Product Data Sheet, 1997) (Figure 2.4.). The packing device and extra sand were removed from the top of the tank, which was then gently tapped to create an even sand surface. A cover was secured around the apparatus to block the refractive and reflective light from the LED source, and to ensure that only transmitted light is seen in the images. Specifically, 1 cm of the top portion of the tank and sand was covered; this dimension is assumed as part of the uniform wetting front for the data presented here.

All tank flow experiments were done in replicate, with data presented in Table 2.3. derived from the averages of the replica, and the images presented from a single experiment representing the system's characteristics (Figures 2.9. – 2.12.). The secondary experimental images are available for viewing in Appendix A. The experimental exudate and soil component solutions were individually pumped into the 2D tank per each experiment. A Cole Parmer peristaltic pump was use for this process (pump head; Masterflex easy loader II L/S model 77200-60, Masterflex peroxide-cured silicone tubing L/S 16, Cole Parmer Instruments Co., Vernon Hills, IL) with the solutions distributed across the top of the 2D tank by artificial rainfall (rotating screw actuator) over a 45.72 cm^2 area, at a constant pump rate of 10 mL/min (flow velocity of 13.12 cm/hr).

A Nikon CMOS D5500 DSLR camera with AF-S DX NIKKOR 18-55mm f/3.5-5.6G VR II Lens (model: 1546) was used to image the flow every 30 seconds in large,

fine, JPEG format, with 6000 × 4000 pixels per image. The camera was operated manually to ensure that the highest intensity within the images was less than the maximum of 255. This was also done for the calibration curve images. Upon capture, the images were imported into Matlab for quantitative analysis. The raw red-green-blue (RGB) formatted images were converted to a hue-saturation-intensity (HSI) format. The intensity values were then used to determine the dynamic finger geometry and the vertical and horizontal water saturation profiles via Matlab (R2016a, The Mathworks Inc., Natick, MA, USA).

2.3. RESULTS

2.3.1. Surface and Interface Characterizations

The dynamic contact angles of each constituent solution at their various concentrations are displayed in Figure 2.5., with the stable contact angle measurements listed in Table 2.3. (stable measurements taken at 90 seconds). For most concentrations of the exudate solutions the contact angles are significantly lower than the NaCl+HNS control solution (64.5 θ at 90 s), the exception being the low concentration of SRNOM. Statistical analysis of the contact angle and surface tension was done via t-test, and the differences are compiled in Table 2.4. Although certain solutions exhibited an excess data overlap which prevents discerning a significant difference in the graph itself, each constituent group displays a percent reduction of the contact angles, seen in Figure 2.6., of the experimental solutions against the control at time 90 s, as well as, illustrates the t-test groupings. The SRNOM percent reduction in the contact angle values were 4% for

0.1 mg/L and 30% for 10 mg/L. The citrate percent reduction in the contact angle values were 18% for 0.1 mg/L and 29% for 500 mg/L. The oxalate percent reduction in the contact angle values were 15% for 0.1 mg/L and 26% for 500 mg/L. For the for tannic acid, however, the variance in the reduction in contact angle regardless of the increase in concentration, thus averaging the percent reduction is to 17%.

Dynamic surface tension measurements were taken at 30 second intervals for all experimental solutions and are displayed in Figure 2.7. Additionally, the stable surface tension measurements (at time 90 s) are listed in Table 2.3., and were used to determine the percent reduction in surface tension, seen in Figure 2.8. All solutions exhibited a lower surface tension than the NaCl+HNS control solution (75.7 mN/m at 90 s). As with the contact angle data, the changes in surface tension were not coupled directly with changes in concentration. For example, in Figures 2.5. and 2.7., the 500 mg/L citrate solution exhibited the lowest contact angle (46 θ) and the highest surface tension (73.6 mN/m), respectively (stable time at 90 s). The percent reduction in surface tension t-test groupings illustrate more specifically the effect of the concentration variations on the surface tension. However, the percent reduction in surface tension for the experimental solutions compared to the control were fairly small, less than 10%. Additionally, the bond number for the solutions was calculated for all of the experimental solutions to fall between 2.7-3.9E-4, illustrating the importance of the surface tension plays in the behavior of the solutions (Table 2.5.). The densities of the experimental solutions were also calculated and found to range minimally, from 995.5 – 1002.8 kg/m^3.

2.3.2 Time Dependent Unstable Fingering Flow

The unsaturated gravity driven flow experiments were analyzed based on i) the number of fingers formed, ii) the velocity of finger propagation, and iii) the vertical and horizontal water saturation profiles. The two extreme concentrations for the plant constituents, which was 0.1 mg/L the lowest and 500 mg/L for the highest were compared with the concentration of the soil constituent, which was 0.1 mg/L to 10 mg/L.

In this comparison, the number of fingers formed in each test varied slightly (1.5 - 2.5 on average) with no discernable pattern between the various constituents and concentrations. Although a variation was observed in the wetting depth of each solution, a relationship to the finger propagation velocity was observed in the citrate, oxalate, and tannic acid solutions. The relationship showed that the slower propagation of the fingers indicated a greater wetting depth (Table 2.3.), which did not hold for the soil constituent SRNOM solutions. The finger length and the wetting depth of the citrate solutions at ten minutes is 22.4 cm and 3.5 cm for the low concentration, and 19.5 and 2.5 cm for the high concentration. The finger length and wetting depth of the SRNOM solutions at ten minutes is 17.7 cm and 7.0 cm for the low concentration, and 13.3 and 3.3 cm for the high concentration. The finger length and wetting depth of the oxalate solutions at ten minutes is 20.2 cm and 3.4 cm for the low concentration and 22.2 and 2.3 cm for the high concentration. The finger length and wetting depth of the tannic acid solutions at ten minutes is 19.1 cm and 4.3 cm for the low concentration and 25.5 and 2.5 cm for the high concentration.

2.3.3. Finger Analysis

Matlab was next used to process and analyze the vertical water saturation profiles of the main finger for each solution (Figures 2.9. & 2.10.). Although the NaCl+HNS control solution exhibited a substantial wetting front and a uniform water distribution through the vertical finger profile, a steady gradient of higher to lower saturation, from the tip of the finger (~90%) to the top of the tank (~50%) was observed. The citrate solutions were similar in that both the 0.1 mg/L and 500 mg/L formed two fingers. However, the 0.1 mg/L citrate solution formed two long and narrow fingers, width of 6.6 cm, with the majority of the water content located directly behind the wetting front (~100%). In juxtaposition, the 500 mg/L citrate solution formed two well-dispersed fingers that were 7.9 cm in width with relatively uniform water saturation profiles (~80%). These well-dispersed water saturation profiles characterized the oxalate solutions, with an average saturation of ~85% for the low and high concentrations. The 0.1 mg/L had a greater finger length, most likely because the two fingers formed in the 0.1 mg/L sample had a width of 8.4 cm, unlike the three fingers with a width of 7.1 cm in the 500 mg/L analysis. Both long and narrow fingers with widths of 7.6 cm were observed forming from the tannic acid 500 mg/L test, with the majority of the water saturation occurring behind the tip of the wetting front (~100%). Further, the tannic acid at 0.1 mg/L had a slightly more uniform water saturation distribution across the finger, with a width of 10.2 cm, though the majority of the saturation still occurred within the fingertip (~75%). Finally, SRNOM exhibited a deep wetting front and uniform water distribution across the finger profiles for both concentrations with only a minimal

variation (~85-88%), though the low-to-high concentrations of the finger widths did vary from 6 cm and 7.5 cm respectively.

The horizontal finger saturation profiles were taken at 25%, 50%, 75%, and 90% of the main fingers length at 10 minutes (Figures 2.11. & 2.12.). The greatest water saturation occurred within the middle finger of the NaCl+HNS control water saturation profile (~85%), which gradually dispersed towards the finger edges (~25-38%). Although both oxalate concentrations exhibited similar saturations in the center of the fingers (~87%), the higher concentration (~40%) had a greater dispersion zone than the lower (~60%). A high level of saturation was observed in the substantial portion of the center of the main finger in the 0.1 mg/L citrate sample (~100%), with a small sharp zone of dispersion (~60%) along the edges of the finger. However, although less saturation (~85%) was observed in the middle of the finger of the 500 mg/L citrate sample, a greater dispersion zone (~40-50%) did manifest along the finger's edge. SRNOM at both concentrations exhibited a similarly high saturation (~88%) in the center of the finger, though the 10 mg/L sample had a smaller zone of dispersion saturation (~50%). Overall, unlike the lower exudate concentrations that exhibited smaller water saturation dispersion zones toward the finger edges, at the higher concentrations, an increase in water saturation was observed through the center of the finger and larger water saturation dispersion zones were observed moving toward the finger edges. Tannic acid responded differently than any of the other constituents, exhibiting lower saturation (~85%) in the middle of the finger and a greater dispersion zone (~60%) at 0.1 mg/L. At 500 mg/L, a

higher saturation (~100%) in the middle of the finger and a smaller dispersion zone (~75%) were observed.

2.4. DISCUSSION

The objective of this study was to elucidate the influence of various plant exudates and soil constituents on the soil infiltration, particularly wetting front instability and fingered flow in unsaturated porous media. By utilizing plant exudate and soil constituent solutions the physical effects of plant root interaction with soil infiltration processes and porous media spatial characteristics, such as heterogeneity and structure, were removed. Only the interactions between the water chemistry, the porous media properties, and the flow dynamics were analyzed for an independent determination of the individual constituent solution effects on the soil infiltration processes that were in the form wetting front instability and fingering flow phenomena.

Unstable fingering flow geometries have been studied under several scenarios, most notably that of Parlange and Hill (1976) who derived modeling equations to predict the width of a finger in an air-water system by incorporating the sorbtivity, and Glass and Nicholl (1996) who adjusted the equation to fit an air-water system. This system is expressed as:

$$d_c = \pi \frac{S^2}{2K_s(\theta_s - \theta_i)} \left(\frac{1}{1 - q_s/K_s}\right) \tag{3}$$

where d_c is the minimum finger width, S is the sorptivity, θ_s is the saturated water content, θ_i is the initial water content, q_s is the flux, K_s is the saturated hydraulic conductivity, and π is a constant for a 2D system (Glass et al., 1991; Wallach et al.,

2013). It is important to note that the intrinsic sorptivity is independent of the liquid properties (Philip, 1969; Wallach et al., 2013).

2.4.1. Infiltration Processes

The abrupt difference in water saturation along the fingers boundary, as observed in the vertical and horizontal water saturation distribution profiles that displayed high water saturation behind the wetting front and dry porous media ahead of the wetting front (Figures 2.9. – 2.12.), can be explained by a reduction in sorbtivity of porous media and therefore involving the contact angle (Philip, 1971). The interplay between the resistance to wetting resulting from contact angle at the wetting front together with saturation overshoot and wetting front propagation is visualized by the vertical and horizontal water saturation distribution profiles that demonstrated in most cases the fingered flow with saturation overshoot (Figures 2.9. and 2.10.) and decrease of contact angle (Figures 2.5. and 2.6.) of all the system tested compared to the control infiltration experiment.

In the initial phase of infiltration process in dry porous media with contact angle close to zero, the wetting front diffuses though the porous media as the capillary forces dominate the gravity forces. Afterwards, as the capillary forces and the gravity forces assume an equal status, the wetting front propagates downward as a traveling wave. As the capillary force decreases from the influence of the contact angle that either substantially differs from zero and/or is lower that the contact angle of the control solution, gravity forces overcome capillary forces. An abrupt wetting front is then generated with a high level of water saturation, which causes the development of an

unstable wetting front that causes the formation of fingered flow. A higher (advancing) contact angle is located at the wetting front that propagates in the porous media and a lower (receding) contact angle is present in the now-wetted porous media (Morrow, 1976). The disproportion between the inward and outward fluxes at the fingertip increases, which results in the development of the overshoot saturation. This increase in water saturation at the fingertip "saturation overshoot" causes a rise in pressure and creates a positive matric potential gradient on top of the fingertip (DiCarlo et al., 1999; Geiger and Durnford, 2000). This rise in pressure also increases the delineation between the wet and dry porous media at the edge of the wetting front and facilitates the propagation of the wetting front. The length of the saturation overshoot (i.e. the fingertip length) was deemed a function of the wetting front velocities (DiCarlo, 2004; Wallach et al., 2013). Our experimental results which include the vertical water distribution profiles, the visualization of the overshoot saturation, and the wetting front velocity measurements definitely support these findings (Figures 2.9. and 2.10.; Table 2.3.).

2.4.2. Redistribution Processes

After the initial infiltration process the redistribution within the fingering flow changes depending upon the simulated constituents and their concentrations. A noticeable effect of the constituents and concentrations upon the water distribution was observed, due to the different matric potentials within the systems. Although this increase in the matric potentials causes "saturation overshoot" (i.e. resulting in saturated fingertips) a reduced matric potential enhances the fluid movement in the porous media with a more

uniform saturation distribution (DiCarlo, 2004; Glass et al., 1989c, 1989d; Wallach et al., 2013). The occurrence "saturation overshoot" at the fingertips occurs was the result of the fingering flow failing to overcome the pressure potential to ensure the downward flow (as seen in Figures 2.9. – 2.12.) most notably in the citrate and tannic acid flow systems. It is possible, however, to use data from the fundamental contact angle and surface tension analysis of the solutions in conjunction with the "saturation overshoot" observations to further illustrate the wettability changes in the flow patterns and the water content distribution of the finger saturation profiles. An increase in wettability causes an increase in solution sorptivity, caused by the reduction in the matric potential required for the solution to enter the pore spaces. The matric pressures for each of the constituent solutions are markedly lower at the higher concentrations than at lower concentrations. These pressure changes present themselves as variations in the water saturation distributions determined elsewhere. Specifically, Wallace et al. (2013) found that for systems with higher contact angles, the air-entry pressure was greater, and thus the fingering flow is most likely to develop a more highly saturated fingertip (the "saturation overshoot") (DiCarlo, 2004; Glass et al., 1989c, 1989d; Wallach et al., 2013). Similar results were determined in this present analysis in which the higher concentration solutions exhibited lower contact angles with more uniform saturation distributions. A comparison between the low and high concentrations for citrate and tannic acid clearly indicated the presence of "saturation overshoot" at lower concentrations when the contact angle was prevalent. At higher concentrations, however, the solution saturation exhibited a greater uniformity with a more substantially reduced contact angle. The results from the

study illustrate an almost linear relationship between the contact angle of a solution and its capillary pressure, specifically in determining a direct correlation between a decreased contact angle and decreased capillary pressure. However, these conclusions cannot be applied to oxalate and SRNOM, which at both concentrations exhibit uniform saturations, illustrating that factors such as flow rate (Wallach et al., 2013), clearly affect the finger geometries and development. Additionally, with limited comparable plant exudate studies, comparisons can be drawn to existing studies upon the effects of surfactants in soil systems since plant exudates act as organic surfactants in the rhizosphere. It was determined that the simulated plant exudates and the soil constituent solutions exhibited behaviors similar to that delineated in the studies of Bashir et al. (2011), and Henry and Smith (2002).

2.4.3. Exudate Effects

The addition of surfactants, biosurfactants, or exudates can alter the solution chemistry enough to produce a change in behavior of a media's hydraulic properties. In their study of hydraulic conductivity and hydrophobicity in root-soil interfaces, Zarebanadkouki et al. (2016) analyzed how wetting and drying cycling affected the hydraulic conductivity and potential hydrophobicity of the soil matric in the rhizosphere (Zarebanadkouki et al., 2016). They concluded that mucilage and exudates were a crucial determinant in conserving water for a plant to use during a drying period. However, after the water stores were depleted, the dried mucilage turned the soil hydrophobic, and remained so even after multiple re-wetting events. Furthermore the hydrophobicity

caused a simultaneous reduction of the hydraulic conductivity of the systems (Zarebanadkouki et al., 2016). Juxtaposing these results that presented in this paper, the exudates, apart from the mucilage component, ultimately exert the opposite impact on flow through the porous media. This increase in the mobility of the fluid through the system, and fluid holding capabilities are illustrated in Figures 2.9. – 2.12.. Specifically, in their study of the effects of plant mucilage and phospholipids on the physical and chemical properties of soil, Read et al. (2003) observed a decrease of the surface tension of the soil water systems brought about by very small concentrations of phospholipid surfactants and exudate organic acids (Read et al., 2003). The increased wettability, and thus, mobility of the soil solution in the porous media is important for further studies to elucidate the transport of contaminants in the vadose zone and rhizosphere.

The rhizosphere is extremely complex, and interactions between the components are typically compounding, as a comparison of the study of Zarebanadkouki et al. (2016) to that of Walker et al. (2003) indicates. Specifically, in the broad approach used to elucidate the entire root system, Walker et al. (2003) found that the root exudates compounded with mucilage under certain circumstances exhibited a stabilizing effect on the rhizosphere. While the exudates lowered the surface tension of the soil pore-water, similar what the authors determined in this research (Figures 2.7. and 2.8.), the mucilage acted as a glue, bonding soil aggregates to the root sheaths and creating a water holding space around the roots as the surrounding soil continued to dry (Walker et al., 2003). The simplicity of solely analyzing the effects of exudates as shown in Figures 2.5. – 2.8., is

beneficial in understanding the separate components of the rhizosphere as they exist (i.e. uncompounded by the rest of the multiple components).

2.4.4. Imaging Capabilities

The recent surge in the development of visualization and modeling capabilities, specifically relating to 2D tanks, has been instrumental in studies attempting to elucidate rhizosphere systems and root zone development and characterization in situ (Carminati et al., 2016). These new capabilities, paired with current biological understandings have yielded a novel understanding of the entire plant-root-soil-water system. However, even with such an acceleration of research, the specific distribution and paths that the fluid takes from the soil matrix into and through the plant itself remains unknown (Carminati et al., 2016). As stated by Carminati et al. (2016), "*Coupling these measurements with imaging techniques that allow visualization of the root architecture and the structure and moisture of the rhizosphere could be the ultimate experiment to measure the rhizosphere properties*". The analysis presented here clearly indicates the effectiveness of combining 2D tank systems with imaging techniques such as LTM to furthering understanding of high special and temporal fluid distribution and moisture gradients in the rhizosphere directly under the influence of plant roots. The increase in sensor sensitivity, particularly of matric potential sensors or pressure transducers, will be of great value in acquiring additional insight to the mechanisms occurring in the rhizosphere.

2.5. CONCLUSION

Dynamic 2D tank flow experiments were coupled with the unique LTM in order to provide a novel analysis of the influence of plant exudate on infiltration flow and wettability in a porous media. This unique approach makes it possible for the rapid and high-resolution quantification of fluid saturation profiles. The primary objective of this research was to investigate the impact of low and high concentrations of simulated plant root exudates and a soil constituent on unstable infiltration flows within a homogenous porous media. Overall, the both concentrations of each constituent were observed to exert a significant effect on the wettability of the fluids when compared to the control. Though no changes were really seen in between the different concentrations or constituents in the flow systems, though, again, a change was seen between the experimental solutions as a whole and the control. Such findings illustrate the point that more normalized, or natural, concentrations of these constituents can significantly impact the wettability of infiltration into the rhizosphere. The data produced here provides the basis for future analysis of the rhizosphere processes, where the natural biochemical concentrations exuded from the roots should be great enough to create significant changes in the mobility and wettability of fluids and anything moving within the root zone. The results developed here will also be of use in increasing the efficiency of agricultural practices related to irrigation application and water management.

Acknowledgements

This material is based upon work supported by the U.S. Department of Energy Office of Science, Office of Basic Energy Sciences and Office of Biological and Environmental Research under Award Number DE-SC-00012530.

REFERENCES

Ahmed, M. A., Kroener, E., Holz, M., Zarebanadkouki, M., & Carminati, A. (2014). Mucilage exudation facilitates root water uptake in dry soils. *Functional Plant Biology*, *41*(10–11), 1129–1137. https://doi.org/10.1071/fp13330

Alami, Y., Achouak, W., Marol, C., & Heulin, T. (2000). Rhizosphere soil aggregation and plant growth promotion of sunflowers by an exopolysaccharide-producing Rhizobium sp strain isolated from sunflower roots. *Applied and Environmental Microbiology*, *66*(8), 3393–3398. https://doi.org/10.1128/aem.66.8.3393-3398.2000

Allaire, S. E., Roulier, S., & Cessna, A. J. (2009). Quantifying preferential flow in soils: A review of different techniques. *Journal of Hydrology*, *378*(1–2), 179–204. https://doi.org/10.1016/j.jhydrol.2009.08.013

Andreini, M. S., & Steenhuis, T. S. (1990). Preferential paths of flow under conventional and conservation tillage. *Geoderma*, *46*(1–3), 85–102. https://doi.org/10.1016/0016-7061(90)90009-X

Assouline, S. (2013). Infiltration into soils: Conceptual approaches and solutions. *Water Resources Research*, *49*(4), 1755–1772. https://doi.org/10.1002/wrcr.20155

Baker, R. S., & Hillel, D. (1991). Observations of fingering behavior during infiltration into layerd soils. *Preferential Flow: Proceedings of the National Symposium*, 87–99.

Bauters, T. W. J., DiCarlo, D. a, Steenhius, T. S., & Parlange, J.-Y. (2000). Soil water content dependent wetting front caracteristics in sands, *232*, 244–254.

Bauters, T. W. ., Steenhuis, T. ., DiCarlo, D. ., Nieber, J. ., Dekker, L. ., Ritsema, C. ., … Haverkamp, R. (2000). Physics of water repellent soils. *Journal of Hydrology*, *231*, 233–243. https://doi.org/10.1016/S0022-1694(00)00197-9

Benard, P., Kroener, E., Vontobel, P., Kaestner, A., & Carminati, A. (2016). Water percolation through the root-soil interface. *Advances in Water Resources*, *95*, 190–198. https://doi.org/10.1016/j.advwatres.2015.09.014

Bengough, a. G. (2012). Water dynamics of the root zone: Rhizosphere biophysics and its control on soil hydrology. *Vadose Zone Journal*, *11*(2), 0. https://doi.org/10.2136/vzj2011.0111

Beven, K., & Germann, P. (2013). Macropores and water flow in soils revisited. *Water Resources Research*, *49*(6), 3071–3092. https://doi.org/10.1002/wrcr.20156

Bien, L. B., Angulo-Jaramillo, R., Predelus, D., Lassabatere, L., & Winiarski, T. (2013). Preferential flow and mass transport modeling in a heterogeneous unsaturated soil. *Advances in Unsaturated Soils*, 211–216.

Bouma, J., & Dekker, L. W. (1978). Case-study on infiltration into dry clay soil.1. Morphological observations. *Geoderma*, *20*(1), 27–40. https://doi.org/10.1016/0016-7061(78)90047-2

Boyer, D. G., Kuczynska, E., & Fayer, R. (2009). Transport, fate, and infectivity of Cryptosporidium parvum oocysts released from manure and leached through macroporous soil. *Environmental Geology*, *58*(5), 1011–1019. https://doi.org/10.1007/s00254-008-1580-x

Buckingham, E. (1907). Studies on the movement of soil moisture. *Bureau of Soils - Bulletin*, *38*.

Bundt, M., Albrecht, A., Froidevaux, P., Blaser, P., & Fluhler, H. (2000). Impact of preferential flow on radionuclide distribution in soil. *Environmental Science & Technology*, *34*(18), 3895–3899. https://doi.org/10.1021/es9913636

Cakmak, I., Erenoglu, B., Gulut, K. Y., Derici, R., & Romheld, V. (1998). Light-mediated release of phytosiderophores in wheat and barley under iron or zinc deficiency. *Plant and Soil*, *202*(2), 309–315. https://doi.org/10.1023/a:1004384712817

Carminati, A. (2012). A model of root water uptake coupled with rhizosphere dynamics. *Vadose Zone Journal*, *11*(3). https://doi.org/10.2136/vzj2011.0106

Carminati, A., Moradi, A. B., Vetterlein, D., Vontobel, P., Lehmann, E., Weller, U., … Oswald, S. E. (2010). Dynamics of soil water content in the rhizosphere. *Plant and Soil*, *332*(1), 163–176. https://doi.org/10.1007/s11104-010-0283-8

Carvalhais, L. C., Dennis, P. G., Fedoseyenko, D., Hajirezaei, M. R., Borriss, R., & Von Wir??n, N. (2011). Root exudation of sugars, amino acids, and organic acids by maize as affected by nitrogen, phosphorus, potassium, and iron deficiency. *Journal of Plant Nutrition and Soil Science*, *174*(1), 3–11. https://doi.org/10.1002/jpln.201000085

Chouke, R. L., van Meurs, P., & van der Poel, C. (1959). The instability of slow immiscible, viscous liquid-liquid displacements in porous media. *Transactions of the American Institute of Mining Engineers*, *216*, 188–194.

Clothier, B. E., Green, S. R., & Deurer, M. (2008). Preferential flow and transport in soil: progress and prognosis. *European Journal of Soil Science*, *59*(1), 2–13. https://doi.org/10.1111/j.1365-2389.2007.00991.x

Cueto-Felgueroso, L., & Juanes, R. (2009). A phase field model of unsaturated flow. *Water Resources Research*, *45*(10), 1–23. https://doi.org/10.1029/2009WR007945

Cueto-Felgueroso, L., & Juanes, R. (2008). Nonlocal interface dynamics and pattern formation in gravity-driven unsaturated flow through porous media. *Physical Review Letters*, *101*(24). https://doi.org/10.1103/PhysRevLett.101.244504

Cueto-Felgueroso, L., Juanes, R., & Asme. (2009). Phase-field models of gravity-driven unsaturated flow in porous media. *Imece 2008: Mechanics of Solids, Structures and Fluids, Vol 12*, 35–40.

Cueto-Felgueroso, L., & Juanes, R. (2009). Stability analysis of a phase-field model of gravity-driven unsaturated flow through porous media. *Physical Review E - Statistical, Nonlinear, and Soft Matter Physics*, *79*(3), 44–47. https://doi.org/10.1103/PhysRevE.79.036301

Czarnes, S., Hallett, P. D., Bengough, A. G., & Young, I. M. (2000). Root- and microbial-derived mucilages affect soil structure and water transport. *European Journal of Soil Science*. https://doi.org/10.1046/j.1365-2389.2000.00327.x

Darnault, C. J. G., Garnier, P., Kim, Y. J., Oveson, K. L., Steenhuis, T. S., Parlange, J. Y., … Baveye, P. (2003). Preferential transport of Cryptosporidium parvum oocysts in variably saturated subsurface environments. *Water Environment Research*, *75*(2), 113–120. https://doi.org/10.2175/106143003X140890

Darnault, C. J. G., Steenhuis, T. S., Garnier, P., Kim, Y. J., Jenkins, M. B., Ghiorse, W. C., … Parlange, J. Y. (2004). Preferential flow and transport of Cryptosporidium parvum oocysts through the vadose zone: Experiments and modeling. *Vadose Zone Journal*, *3*(1), 262–270.

De Rooij, G. H. (2000). Modeling fingered flow of water in soils owing to wetting front instability: A review. *Journal of Hydrology*, *231–232*, 277–294. https://doi.org/10.1016/S0022-1694(00)00201-8

Dekker, L. W., & Ritsema, C. J. (1994). How water moves in a water repellent sany soil .1. Potential and actual water repellency. *Water Resources Research*, *30*(9), 2507–2517. https://doi.org/10.1029/94wr00749

DiCarlo, D. A. (2004). Experimental measurements of saturation overshoot on infiltration. *Water Resources Research*, *40*(4). https://doi.org/10.1029/2003wr002670

DiCarlo, D. A., Bauters, T. W. J., Darnault, C. J. G., Steenhuis, T. S., & Parlange, J. Y. (1999). Lateral expansion of preferential flow paths in sands. *Water Resources Research*, *35*(2), 427–434. https://doi.org/10.1029/1998wr900061

Diment, G. A., & Watson, K. K. (1985). Stability analysis of water movement in unsaturated porous materials: 3. Experimental studies. *Water Resources Research*, *21*(7), 979–984. https://doi.org/10.1029/WR021i007p00979

Dorr, H., & Munnich, K. O. (1991). Lead and cesium transport in european forest soils. *Water Air and Soil Pollution*, *57–8*, 809–818. https://doi.org/10.1007/bf00282944

Dresel, P. E., Wellman, D. M., Cantrell, K. J., & Truex, M. J. (2011). Review: Technical and policy challenges in deep vadose zone remediation of metals and radionuclides. *Environmental Science & Technology*, *45*(10), 4207–4216. https://doi.org/10.1021/es101211t

Egorov, A. G., Dautov, R. Z., Nieber, J. L., & Sheshukov, A. Y. (2003). Stability analysis of gravity-driven infiltrating flow. *Water Resources Research*, *39*(9). https://doi.org/10.1029/2002wr001886

Engelhardt, I., Sittig, S., Simunek, J., Groeneweg, J., Putz, T., & Vereecken, H. (2015). Fate of the antibiotic sulfadiazine in natural soils: Experimental and numerical investigations. *Journal of Contaminant Hydrology*, *177*, 30–42. https://doi.org/10.1016/j.jconhyd.2015.02.006

Flury, M., Fluhler, H., Jury, W. A., & Leuenberger, J. (1994). Susceptibility of soils to preferential flow of water - A field-study. *Water Resources Research*, *30*(7), 1945–1954. https://doi.org/10.1029/94wr00871

Gardner, W. R. (1960). Dynamic aspects of water availability to plants. *Soil Sci*, *89*((2)), 63–73.

Geiger, S. L., & Durnford, D. S. (2000). Infiltration in homogeneous sands and a mechanistic model of unstable flow. *Soil Science Society of America Journal*, *64*(2), 460–469.

Gerke, H. H., Germann, P., & Nieber, J. (2010). Preferential and unstable flow: From the pore to the catchment scale. *Vadose Zone Journal*, *9*(2), 207–212. https://doi.org/10.2136/vzj2010.0059

Ghezzehei, T. A., & Albalasmeh, A. A. (2015). Spatial distribution of rhizodeposits provides built-in water potential gradient in the rhizosphere. *Ecological Modelling*, *298*, 53–63. https://doi.org/10.1016/j.ecolmodel.2014.10.028

Glass, R. J., Oosting, G. H., & Steenhuis, T. S. (1989). Preferential solute transport in layered homogeneous sands as a consequence of wetting front instability. *Journal of Hydrology*, *110*(1–2), 87–105. https://doi.org/10.1016/0022-1694(89)90238-2

Glass, R. J., Parlange, J.-Y., & Steenhuis, T. S. (1991). Immiscible displacement in porous media: Stability analysis of three-dimensional, axisymmetric disturbances with application to gravity-driven wetting front instability. *Water Resources Research*, *27*(8), 1947–1956. https://doi.org/10.1029/91WR00836

Glass, R. J., & Nicholl, M. J. (1996). Physics of gravity fingering of immiscible fluids within porous media: An overview of current understanding and selected complicating factors. *Geoderma*, *70*(2–4), 133–163. https://doi.org/10.1016/0016-7061(95)00078-X

Glass, R. J., Parlange, J.-Y., & Steenhuis, T. S. (1989). Wetting front instability: 1. Theoretical discussion and dimensional analysis. *Water Resources Research*, *25*(6), 1187–1194.

Glass, R. J., Steenhuis, T. S., & Parlange, J.-Y. (1989). Wetting front instability: 2. Experimental determination of relationships between system parameters and two-dimensional unstable flow field behavior in initially dry porous media. *Water Resources Research*, *25*(6), 1195–1207.

Glass, R. J., Steenhuis, T. S., & Parlange, J.-Y. (1989). Mechanism for finger persistence in homogeneous, unsaturated, porous media: Theory and verification. *Soil Science*, *148*(1), 60–70.

Gregory, P. J. (2006). Roots, rhizosphere and soil: The route to a better understanding of soil science? *European Journal of Soil Science*, *57*(1), 2–12. https://doi.org/10.1111/j.1365-2389.2005.00778.x

Guinel, F. C., & McCully, M. E. (1986). Some water-related physical properties of maize root-cap mucilage. *Plant Cell and Environment*, *9*(8), 657–666. https://doi.org/10.1111/j.1365-3040.1986.tb01624.x

Hallett, P. D., Karim, K. H., Bengough, A. G., & Otten, W. (2013). Biophysics of the vadose zone: From reality to model systems and back again. *Vadose Zone Journal*, *12*(4). https://doi.org/10.2136/vzj2013.05.0090

Hendrickx, J. M. H., & Flury, M. (2001). Uniform and preferential flow mechanisms in the vadose zone. *Conceptual Models of Flow and Transport in the Fractured Vadose zone.Natl.Acad.Press, Washington, DC*, 149–187. https://doi.org/doi:10.17226/10102

Hill, D. E., & Parlange, J.-Y. (1972). Wetting front instability in layered soils. *Soil Science Society of America Journal*, *36*(5), 697–702.

Hillel, D. (1987). Unstable flow in layered soils - A review. *Hydrological Processes*, *1*(2), 143–147. https://doi.org/10.1002/hyp.3360010203

Hinsinger, P., Bengough, A. G., Vetterlein, D., & Young, I. M. (2009). Rhizosphere: biophysics, biogeochemistry and ecological relevance. *Plant and Soil*, *321*(1–2), 117–152. https://doi.org/10.1007/s11104-008-9885-9

Hoa, N. T. (1981). A new method allowing the measurement of rapid variations of the water content in sandy porous media. *Water Resources Research*, *17*(1), 41–48. https://doi.org/10.1029/WR017i001p00041

Homsy, G. M. (1987). Viscous fingering in porous media. *Annual Review of Fluid Mechanics*, *19*, 271–311. https://doi.org/10.1146/annurev.fluid.19.1.271

Horton, R. E. (1933). The role of infiltration in the hydrologic cycle. *Transactions, American Geophysical Union*, *14*, 446–460.

Jarvis, N. J. (2007). A review of non-equilibrium water flow and solute transport in soil macropores: Principles, controlling factors and consequences for water quality. *European Journal of Soil Science*. https://doi.org/10.1111/j.1365-2389.2007.00915.x

Jarvis, N., Koestel, J., & Larsbo, M. (2016). Understanding preferential flow in the vadose zone: Recent advances and future prospects. *Vadose Zone Journal*, *15*(12), 0. https://doi.org/10.2136/vzj2016.09.0075

Jones, D. (1998). Organic acids in the rhizosphere: A critical review. *Plant and Soil*, *205*, 25–44. https://doi.org/10.1023/A:1004356007312

Jones, T. E., Wood, M. I., Corbin, R. A., & Simpson, B. C. (2001). *Preliminary inventory estimates for single-shell tank leaks in B, BX, and BY tank farms*. Richland, WA.

Kaci, Y., Heyraud, A., Barakat, M., & Heulin, T. (2005). Isolation and identification of an EPS-producing Rhizobium strain from and soil (Algeria): Characterization of its EPS and the effect of inoculation on wheat rhizosphere soil structure. *Research in Microbiology*, *156*(4), 522–531. https://doi.org/10.1016/j.resmic.2005.01.012

Kapoor, V. (1996). Criterion for instability of steady-state unsaturated flows. *Transport in Porous Media*, *25*(3), 313–334. https://doi.org/10.1007/bf00140986

Kay, P., Blackwell, P. A., & Boxall, A. B. A. (2004). Fate of veterinary antibiotics in a macroporous tile drained clay soil. *Environmental Toxicology and Chemistry*, *23*(5), 1136–1144. https://doi.org/10.1897/03-374

Kay, P., Blackwell, P. A., & Boxall, A. B. A. (2005). Column studies to investigate the fate of veterinary antibiotics in clay soils following slurry application to agricultural land. *Chemosphere*, *60*(4), 497–507. https://doi.org/10.1016/j.chemosphere.2005.01.028

Kim, Y.-J., Darnault, C. J. G., Bailey, N. O., Parlange, J., & Steenhuis, T. S. (2005). Equation for describing solute transport in field soils with preferential flow paths. *Soil Science Society of America Journal*, *69*(2), 291–300. https://doi.org/10.1084/jem.20070109

Klos, R. A., Simon, I., Bergstrom, U., de Haag, A. M. U., Valentin-Ranc, C., Zeevaert, T., … Stansby, J. (1999). Complementary studies: Biosphere modelling for dose assessments of radioactive waste repositories. *Journal of Environmental Radioactivity*, *42*(2–3), 237–254.

Kung, K. J. S. (1990). Preferential flow in a sandy vadose zone.2. Mechanism and implications. *Geoderma*, *46*(1–3), 59–71. https://doi.org/10.1016/0016-7061(90)90007-v

Kung, K. J. S. (1990). Preferential flow in a sandy vadose zone .1. Field observation. *Geoderma*, *46*(1–3), 51–58. https://doi.org/10.1016/0016-7061(90)90006-u

Laplace, P. S. (1806). *Trait é Méchanique Céleste*. Paris NV - 5: Imprimerie de Crapelet.

Lehmann, P., Neuweiler, I., Vanderborght, J., & Vogel, H. J. (2012). Dynamics of fluid interfaces and flow and transport across material interfaces in porous media-modeling and observations. *Vadose Zone Journal*, *11*(3). https://doi.org/10.2136/vzj2012.0105

Liang, X., Lettenmaier, D. P., Wood, E. F., & Burges, S. J. (1994). A simple hydrologically based model of land-surface water and energy fluxes for general circulation models. *Journal of Geophysical Research-Atmospheres*, *99*(D7), 14415–14428. https://doi.org/10.1029/94jd00483

Liu, Y. P., Steenhuis, T. S., & Parlange, J. Y. (1994). Formation and persistence of fingered flow-fields in coarse-grained soils under different moisture contents.

Journal of Hydrology, *159*(1–4), 187–195. https://doi.org/10.1016/0022-1694(94)90255-0

Lu, T. X., Biggar, J. W., & Nielsen, D. R. (1994). Water movement in glass bead porous media.2. Experiments of infiltration and finger flow. *Water Resources Research*, *30*(12), 3283–3290. https://doi.org/10.1029/94wr00998

McBride, M. B. (1998). Growing food crops on sludge-amended soils: Problems with the US Environmental Protection Agency method of estimating toxic metal transfer. *Environmental Toxicology and Chemistry*, *17*(11), 2274–2281. https://doi.org/10.1897/1551-5028(1998)017<2274:gfcosa>2.3.co;2

McCully, M. E., & Boyer, J. S. (1997). The expansion of maize root-cap mucilage during hydration .3. Changes in water potential and water content. *Physiologia Plantarum*, *99*(1), 169–177. https://doi.org/10.1034/j.1399-3054.1997.990123.x

McCully, M. E. (1999). Roots in soil: Unearthing the complexities of roots and their rhizospheres. *Annual Review of Plant Physiology and Plant Molecular Biology*, *50*(1), 695–718. https://doi.org/10.1146/annurev.arplant.50.1.695

Moradi, A. B., Carminati, A., Lamparter, A., Woche, S. K., Bachmann, J., Vetterlein, D., … Oswald, S. E. (2012). Is the rhizosphere temporarily water repellent? *Vadose Zone Journal*, *11*(3). https://doi.org/10.2136/vzj2011.0120

Moradi, A. B., Carminati, A., Vetterlein, D., Vontobel, P., Lehmann, E., Weller, U., … Oswald, S. E. (2011). Three-dimensional visualization and quantification of water content in the rhizosphere. *New Phytologist*, *192*(3), 653–663. https://doi.org/10.1111/j.1469-8137.2011.03826.x

Morrow, N. R. (1976). Capillary-pressure correlations for uniformly wetted porous media. *Journal of Canadian Petroleum Technology*, *15*(4), 49–69.

Muller, H., & Prohl, G. (1993). ECOSYS-87-A dynamic model for assessing radiological consequences of nuclear accidents. *Health Physics*, *64*(3), 232–252. https://doi.org/10.1097/00004032-199303000-00002

Niemet, M. R., & Selker, J. S. (2001). A new method for quantification of liquid saturation in 2D translucent porous media systems using light transmission. *Advances In Water Resources*, *24*(6), 651–666.

Nimmo, J. R. (2012). Preferential flow occurs in unsaturated conditions. *Hydrological Processes*, *26*(5), 786–789. https://doi.org/10.1002/hyp.8380

Parlange, J. Y. (1971). Theory of water movement in soils.1. One-dimensional absorption. *Soil Science*, *111*(2), 134-. https://doi.org/10.1097/00010694-197102000-00010

Parlange, J. Y. (1973). Theory of water movement in soils.10. Cavities with constant flux. *Soil Science*, *116*(1), 1–7. https://doi.org/10.1097/00010694-197307000-00001

Parlange, J. Y. (1972). Theory of water movement in soils.5. Unsteady infiltration from spherical cavities. *Soil Science*, *113*(3), 156-. https://doi.org/10.1097/00010694-197203000-00002

Parlange, J. Y. (1971). Theory of water movement in soils.3. Two and three-dimensional absorption. *Soil Science*, *112*(5), 313-. https://doi.org/10.1097/00010694-197111000-00003

Parlange, J. Y. (1972). Theory of water movement in soils .4. Two and three-dimensional steady infiltration. *Soil Science*, *113*(2), 96-. https://doi.org/10.1097/00010694-197202000-00004

Parlange, J. Y. (1971). Theory of water movement in soils.2. One-dimensional infiltration. *Soil Science*, *111*(3), 170-. https://doi.org/10.1097/00010694-197103000-00004

Parlange, J. Y. (1972). Theory of water movement in soils .8. One-dimensional infiltration with constant flux at surface. *Soil Science*, *114*(1), 1-.

Parlange, J. Y. (1975). Theory of water movement in soils.11. Conclusion and discussion of some recent developments. *Soil Science*, *119*(2), 158–161. https://doi.org/10.1097/00010694-197502000-00008

Parlange, J. Y. (1972). Theory of water movement in soils .7. Multidimensional cavities under pressure. *Soil Science*, *113*(6), 379-. https://doi.org/10.1097/00010694-197206000-00013

Parlange, J. Y. (1972). Theory of water movement in soils .6. Effect of water depth over soil. *Soil Science*, *113*(5), 308-.

Parlange, J. Y., & Aylor, D. (1972). Theory of water movement in soils .9. Dynamics of capillary rise. *Soil Science*, *114*(2), 79-. https://doi.org/10.1097/00010694-197208000-00001

Passioura, J. B. (1988). Water transport in and to roots. *Annual Review of Plant Physiology and Plant Molecular Biology*, *39*(1), 245–265. https://doi.org/10.1146/annurev.pp.39.060188.001333

Peck, A. J. (1965). Moisture profile development and air compression during water uptake by bounded porous bodies. 3. Vertical columns. *Soil Sci*, *100*((1)), 44–51.

Pendexter, W. S., & Furbish, D. J. (1991). *Development of a heterogeneous moisture distribution and its influence on the evolution of preferred pathways of flow in an unsaturated sandy soil*. (T. J. Gish & A. Shirmohammadi, Eds.), *Preferential Flow: Proceedings of the National Symposium*.

Philip, J. R. (1971). Limitations on scaling by contact angle. *Soil Science Society of America Proceedings*, *35*(3), 507-.

Philip, J. R. (1969). Theory of infiltration. *Advances in Hydroscience*, *5*, 215–296.

Philip, J. R. (1975). Stability analysis of infiltration. *Soil Science Society of America Journal*, *39*(6), 1042–1049.

Qafoku, N. P., Ainsworth, C. C., Szecsody, J. E., & Qafoku, O. S. (2004). Transport-controlled kinetics of dissolution and precipitation in the sediments under alkaline and saline conditions. *Geochimica Et Cosmochimica Acta*, *68*(14), 2981–2995. https://doi.org/10.1016/j.gca.2003.12.017

Raats, P. A. C. (1973). Unstable wetting fronts in uniform and nonuniform soils. *Soil Science Society of America Journal*, *37*(5), 681–685.

Read, D. B., Bengough, A. G., Gregory, P. J., Crawford, J. W., Robinson, D., Scrimgeour, C. M., … Zhang, X. (2003). Plant roots release phospholipid surfactants that modify the physical and chemical properties of soil. *New Phytologist*, *157*(2), 315–326. https://doi.org/10.1046/j.1469-8137.2003.00665.x

Richards, L. A. (1931). Capillary conduction of liquids through porous mediums. *Physics-a Journal of General and Applied Physics*, *1*(1), 318–333. https://doi.org/10.1063/1.1745010

Ritsema, C. J., & Dekker, L. W. (1994). How water moves in a water repellent sandy soil .2. Dynamics of fingered flow. *Water Resources Research*, *30*(9), 2519–2531. https://doi.org/10.1029/94wr00750

Ritsema, C. J., Dekker, L. W., Hendrickx, J. M. H., & Hamminga, W. (1993). Preferential flow mechanism in a water repellent sandy soil. *Water Resources Research*, *29*(7), 2183–2193. https://doi.org/10.1029/93wr00394

Rod, K. A., Um, W., & Flury, M. (2010). Transport of strontium and sesium in simulated Hanford tank waste leachate through quartz sand under saturated and unsaturated

flow. *Environmental Science & Technology*, *44*(21), 8089–8094. https://doi.org/10.1021/es903223x

Rodriguez-Iturbe, I., D'Odorico, P., Porporato, A., & Ridolfi, L. (1999). On the spatial and temporal links between vegetation, climate, and soil moisture. *Water Resources Research*, *35*(12), 3709–3722. https://doi.org/10.1029/1999wr900255

Saffman, P. G. (1986). Viscous fingering in Hele-Shaw cells. *Journal of Fluid Mechanics*, *173*, 73–94. https://doi.org/10.1017/s0022112086001088

Saffman, P. G., & Taylor, G. (1958). The penetration of a fluid into a porous medium or Hele-Shaw cell containing a more viscous liquid. *Proceedings of the Royal Society of London Series a-Mathematical and Physical Sciences*, *245*(1242), 312-. https://doi.org/10.1098/rspa.1958.0085

Selker, J. S., Steenhuis, T. S., & Parlange. (1992). Wetting front instability in homogeneous sandy soils under continuous infiltration. *Soil Science Society of America Journal*, *56*(5), 1346–1350.

Selker, J., Leclerq, P., Parlange, J. Y., & Steenhuis, T. (1992). Fingered flow in two dimensions.1. Measurement of matric potential. *Water Resources Research*, *28*(9), 2513–2521. https://doi.org/10.1029/92wr00963

Selker, J., Parlange, J. Y., & Steenhuis, T. (1992). Fingered flow in two dimensions.2. Predicting finger moisture profile. *Water Resources Research*, *28*(9), 2523–2528. https://doi.org/10.1029/92wr00962

Sililo, O. T. N., & Tellam, J. H. (2000). Fingering in unsaturated zone flow: A qualitative review with laboratory experiments on heterogeneous systems. *Ground Water*, *38*(6), 864–871. https://doi.org/10.1111/j.1745-6584.2000.tb00685.x

Simunek, J., Jarvis, N. J., van Genuchten, M. T., & Gardenas, A. (2003). Review and comparison of models for describing non-equilibrium and preferential flow and transport in the vadose zone. *Journal of Hydrology*, *272*(1–4), 14–35.

Smith, J. T., & Elder, D. G. (1999). A comparison of models for characterizing the distribution of radionuclides with depth in soils. *European Journal of Soil Science*, *50*(2), 295–307. https://doi.org/10.1046/j.1365-2389.1999.00233.x

Steenhuis, T. S., Staubitz, W., Andreini, M. S., Surface, J., Richard, T. L., Paulsen, R., … Geohring, L. D. (1990). Preferential movement of pesticides and tracers in agricultural soils. *Journal of Irrigation and Drainage Engineering-Asce*, *116*(1), 50–66. https://doi.org/10.1061/(asce)0733-9437(1990)116:1(50)

Stokes, J. P., Weitz, D. A., Gollub, J. P., Dougherty, A., Robbins, M. O., Chaikin, P. M., & Lindsay, H. M. (1986). Inerfacial stability of immiscible displacement in a porous medium. *Physical Review Letters*, *57*(14), 1718–1721. https://doi.org/10.1103/PhysRevLett.57.1718

Strobel, B. W. (2001). Influence of vegetation on low-molecular-weight carboxylic acids in soil solution—A review. *Geoderma*, *99*(3–4), 169–198. https://doi.org/10.1016/S0016-7061(00)00102-6

Tamai, N., Asaeda, T., & Jeevaraj, C. G. (1987). Fingering in two-dimensional, homogeneous, unsaturated porous media. *Soil Science*, *144*(2), 107–112.

Tanveer, S. (1987). Analytic theory for the selection of a symmetrical Saffman-Taylor fingering in a Hele-Shaw cell. *Physics of Fluids*, *30*(6), 1589–1605. https://doi.org/10.1063/1.866225

Tanveer, S. (1987). Analytic theory for the linear-stability of the Saffman-Taylor finger. *Physics of Fluids*, *30*(8), 2318–2329. https://doi.org/10.1063/1.866122

Tompson, A. F. B., Hudson, G. B., Smith, D. K., & Hunt, J. R. (2006). Analysis of radionuclide migration through a 200-m vadose zone following a 16-year infiltration event. *Advances in Water Resources*, *29*(2), 281–292. https://doi.org/10.1016/j.advwatres.2005.02.015

Triplett, M. B., Freshley, M. D., Truex, M. J., Wellman, D. M., Gerdes, K. D., Charboneau, B. L., … Asme. (2011). *Integrated strategy to address Hanford's deep vadose zone remediation challenges*. *Proceedings of the 13th International Conference on Environmental Remediation and Radioactive Waste Management, 2010, Vol 2*.

Um, W., Icenhower, J. P., Brown, C. F., Serne, R. J., Wang, Z., Dodge, C. J., & Francis, A. J. (2010). Characterization of uranium-contaminated sediments from beneath a nuclear waste storage tank from Hanford, Washington: Implications for contaminant transport and fate. *Geochimica Et Cosmochimica Acta*, *74*(4), 1363–1380. https://doi.org/10.1016/j.gca.2009.11.014

Um, W., Wang, Z., Serne, R. J., Williams, B. D., Brown, C. F., Dodge, C. J., & Francis, A. J. (2009). Uranium phases in contaminated sediments below Hanford's U Tank Farm. *Environmental Science & Technology*, *43*(12), 4280–4286. https://doi.org/10.1021/es900203r

Uyusur, B., Darnault, C. J. G., Snee, P. T., Koken, E., Jacobson, A. R., & Wells, R. R. (2010). Coupled effects of solution chemistry and hydrodynamics on the mobility and transport of quantum dot nanomaterials in the vadose zone. *Journal of*

Contaminant Hydrology, *118*(3–4), 184–198. https://doi.org/10.1016/j.jconhyd.2010.09.013

Uyusur, B., Li, C. Y., Baveye, P. C., & Darnault, C. J. G. (2015). pH-dependent reactive transport of uranium(VI) in unsaturated sand. *Journal of Soils and Sediments*, *15*(3), 634–647. https://doi.org/10.1007/s11368-014-1018-x

van Meurs, P. (1957). The use of transparent three-dimensional models for studying the mechanism of flow processes in oil reserviors. *Transactions of the American Institute of Mining and Metallurgical Engineers*, *210*(10), 295–301.

van Ommen, H. C., Dijksma, R., Hendrickx, J. M. H., Dekker, L. W., Hulshof, J., & Vandenheuvel, M. (1989). Experimental assessment of preferential flow paths in a field soil. *Journal of Hydrology*, *105*(3–4), 253–262. https://doi.org/10.1016/0022-1694(89)90107-8

Waichler, S. R., & Yabusaki, S. B. (2005). *Flow and transport in the Hanford 300 Area vadose zone-aquifer-river system*. Richland, WA.

Walker, T. S., Bais, H. P., Grotewold, E., & Vivanco, J. M. (2003). Root exudation and rhizosphere biology. *Plant Physiology*, *132*(1), 44–51. https://doi.org/10.1104/pp.102.019661

Wang, K., Zhang, R. D., & Yasuda, H. (2006). Characterizing heterogeneity of soil water flow by dye infiltration experiments. *Journal of Hydrology*, *328*(3–4), 559–571. https://doi.org/10.1016/j.jhydrol.2006.01.001

Wang, X., Tang, C., Guppy, C. N., & Sale, P. W. G. (2008). Phosphorus acquisition characteristics of cotton (Gossypium hirsutum L.), wheat (Triticum aestivum L.) and white lupin (Lupinus albus L.) under P deficient conditions. *Plant and Soil*, *312*(1–2), 117–128. https://doi.org/10.1007/s11104-008-9589-1

Wang, Z., Feyen, J., van Genuchten, M. T., & Nielsen, D. R. (1998). Air entrapment effects on infiltration rate and flow instability. *Water Resources Research*, *34*(2), 213–222. https://doi.org/10.1029/97wr02804

Wang, Z., Jury, W. A., Tuli, A., & Kim, D. J. (2004). Unstable flow during redistribution: Controlling factors and practical implications. *Vadose Zone Journal*, *3*(2), 549–559.

Wang, Z., Tuli, A., & Jury, W. A. (2003). Unstable flow during redistribution in homogeneous soil. *Vadose Zone Journal*, *2*(1), 52–60.

Wang, Z., Wu, L. S., Harter, T., Lu, J. H., & Jury, W. A. (2003). A field study of unstable preferential flow during soil water redistribution. *Water Resources Research*, *39*(4). https://doi.org/Artn 1075\rDoi 10.1029/2001wr000903

Watt, M., McCully, M. E., & Canny, M. J. (1994). Formation and stabilization of rhizosheaths of Zea-Mays L - Effect of soil water content. *Plant Physiology*, *106*(1), 179–186.

Weiler, M. (2017). Macropores and preferential flow-a love-hate relationship. *Hydrological Processes*, *31*(1), 15–19. https://doi.org/10.1002/hyp.11074

Wellman, D. M., Mattigod, S. V, Hubbard, S., Miracle, A., Zhong, L. R., Foote, M., … Asme. (2011). *Advanced remedial methods for metals and radionuclides in vadose zone environments*. *Proceedings of the 13th International Conference on Environmental Remediation and Radioactive Waste Management, 2010, Vol 2*.

White, I., Colombera, P. M., & Philip, J. R. (1977). Experimental studies of wetting front instability induced by gradual change of pressure-gradient and by heterogeneous porous media. *Soil Science Society of America Journal*, *41*(3), 483–489.

White, I., Colombera, P. M., & Philip, J. R. (1976). Experimental study of wetting front instability induced by sudden change of pressure-gradient. *Soil Science Society of America Journal*, *40*(6), 824–829.

Xiong, Y. W. (2014). Flow of water in porous media with saturation overshoot: A review. *Journal of Hydrology*, *510*, 353–362. https://doi.org/10.1016/j.jhydrol.2013.12.043

Yao, T., & Hendrickx, J. M. H. (2001). Stability analysis of the unsaturated water flow equation: 2. Experimental verification. *Water Resources Research*, *37*(7), 1875–1881. https://doi.org/10.1029/2001WR900003

Yao, T., & Hendrickx, J. M. (1996). Stability of wetting fronts in dry homogeneous soils under low infiltration rates. *Soil Science Society of America Journal*, *60*(1), 20–28.

Young, I. M. (1995). Variation in moisture contents between bulk soil and the rhizosheath of wheat (Triticum-Aestivum L CV Wembley). *New Phytologist*, *130*(1), 135–139. https://doi.org/10.1111/j.1469-8137.1995.tb01823.x

Young, T. (1805). An essay on the cohesion of fluids. *Philosophical Transactions of the Royal Society of London*, *95*, 65–87.

Zarebanadkouki, M., Ahmed, M. A., & Carminati, A. (2016). Hydraulic conductivity of the root-soil interface of lupin in sandy soil after drying and rewetting. *Plant and Soil*, *398*(1–2), 267–280. https://doi.org/10.1007/s11104-015-2668-1

Zhang, Y. H., Zhang, M. X., Niu, J. Z., & Zheng, H. J. (2016). The preferential flow of soil: A widespread phenomenon in pedological perspectives. *Eurasian Soil Science*, *49*(6), 661–672. https://doi.org/10.1134/s1064229316060120

TABLES

Table 2.1. Composition of Hoagland Nutrient Solution, recipe followed from Arnon and Hoagland (1940).

	Amount in volume (mL)	Chemical	
Main Solution (creates 1 L of solution)	10	0.5 M $Ca(NO_3)_2$	Calcium nitrate tetrahydrate
	10	0.5 M KNO_3	Potassium nitrate
	4	0.5 M $MgSO_4$	Magnesium sulfate
	2	0.5 M KH_2PO_4	Potassium dihydrogen phosphate
	2	Micronutrient Solution	
Micronutrient Solution (creates 500 mL of solution)	Amount in mass (g)	Chemical	
	1.43	H_3BO_3	Boric acid
	0.9	$MnCl_2$	Manganese(II) chloride
	0.11	$ZnSO_4$	Zinc sulfate concentrate
	0.04	CuSO4	Copper (II) sulfate
	0.1	$(NH_4)_6Mo_7O_{24}$	Ammonium molybdate
	0.28	$FeSO_4$	Iron(II) sulfate heptahydrate
	0.3	EDTA	Edetic acid

Table 2.2. Concentration variations of constituents used to create the solutions tested in this work. Red indicates high concentrations of the constituent, yellow indicates a moderately high amount, and green indicates a typical natural concentration.

Concentration	Citrate (mg/L)	Oxalate (mg/L)	SRNOM (mg/L)	Tannic Acid (mg/L)
High	500	500	-	500
	-	-	10	-
Low	0.1	0.1	0.1	0.1

Table 2.3. Compiled average experimental data from the triplicate fundamental interfacial characterization and the duplicate flow experiments.

	Solution (mg/L)	Average Contact Angle (θ)		Average Surface Tension (mN/m)		Time (sec)	Average Number of Fingers	Average Velocity cm/sec)	Average Wetting Depth (cm)	Average Length (cm)	Average Finger Width (cm)
10 minute Finger Averages	NaCl+HNS	64.5	±2.6	75.8	±0.5	600	4	0.03	6.1	17.3	7.7
	Citrate 500	46.0	±4.9	73.6	±1.1	600	2	0.03	2.5	19.5	7.2
	Citrate 0.1	52.6	±2.3	70.8	±0.4	600	1.5	0.04	3.5	22.4	6.1
	Oxalate 500	47.3	±2.3	71.6	±0.6	600	2.5	0.04	2.3	22.2	7.0
	Oxalate 0.1	54.8	±0.6	73.1	±0.4	600	2.5	0.03	3.4	20.2	7.4
	Tannic Acid 500	54.4	±2.7	70.8	±0.3	600	2	0.04	2.5	25.5	7.5
	Tannic Acid 0.1	52.3	±1.2	72.7	±0.4	600	2	0.03	4.3	19.1	7.8
	Organics 10	45.0	±2.6	73.4	±0.4	600	2	0.02	3.3	13.3	6.0
	Organics 0.1	61.7	±2.6	71.1	±0.2	600	2.5	0.03	7.0	17.7	6.6
Fully Formed Finger Averages	NaCl+HNS	64.5	±2.6	75.8	±0.5	945	4	0.03	8.1	28.8	9.2
	Citrate 500	46.0	±4.9	73.6	±1.1	840	2	0.04	3.9	29.5	7.9
	Citrate 0.1	52.6	±2.3	70.8	±0.4	750	1.5	0.04	3.5	29.5	6.6
	Oxalate 500	47.3	±2.3	71.6	±0.6	720	2.5	0.04	2.3	27.5	7.1
	Oxalate 0.1	54.8	±0.6	73.1	±0.4	825	2	0.03	3.4	27.9	8.4
	Tannic Acid 500	54.4	±2.7	70.8	±0.3	660	1.5	0.05	2.5	29.9	7.6
	Tannic Acid 0.1	52.3	±1.2	72.7	±0.4	930	2	0.03	5.5	27.8	10.2
	Organics 10	45.0	±2.6	73.4	±0.4	975	2	0.03	5.0	29.2	6.0
	Organics 0.1	61.7	±2.6	71.1	±0.2	870	2.5	0.03	9.8	25.7	7.5

Table 2.4. Statistical analysis summary table for t-test significant differentiations.

Solution	Contact Angle (@90s)	Surface Tension (@90s)	# Fingers (@10min)	Velocity (cm/sec) (@10min)	Wetting Depth (cm) (@10min)	Length (cm) (@10min)	Avg Width (cm) (@10min)	# Fingers (@full)	Velocity (cm/sec)(@full)	Wetting Depth (cm) (@full)	Length (cm) (@full)	Avg Width (cm) (@full)
Control	A	A	A	AB	AB	AB	A	A	B	AB	A	AB
CitrateHigh	D	B	B	AB	AB	AB	A	B	AB	BC	A	C
CitrateLow	BC	C	B	AB	AB	AB	A	B	AB	BC	A	ABC
OxalateHigh	CD	C	B	AB	AB	AB	A	B	AB	BC	AB	ABC
OxalateLow	B	B	C	AB	B	AB	A	B	AB	C	AB	BC
TannicHigh	B	C	B	AB	AB	AB	A	B	B	ABC	AB	A
TannicLow	BC	B	B	A	AB	A	A	B	A	BC	A	BC
OrganicHigh	D	B	B	AB	A	AB	A	B	B	A	A	BC
OrganicLow	A	C	B	B	AB	B	A	B	B	ABC	B	C

Table 2.5. Experimental solution densities and bond numbers. Reported numbers are the averages of triplicates.

Solution	Average Density (kg/m^3)	Bond Number
Control	997.6	2.90E-04
Citrate High	996.8	2.99E-04
Citrate Low	999.3	3.11E-04
Oxalate High	1002.8	3.09E-04
Oxalate Low	997.2	3.01E-04
Tannic Acid High	1000.2	3.11E-04
Tannic Acid Low	998.5	3.03E-04
SRNOM High	998.3	3.00E-04
SRNOM Low	995.5	3.09E-04

FIGURES

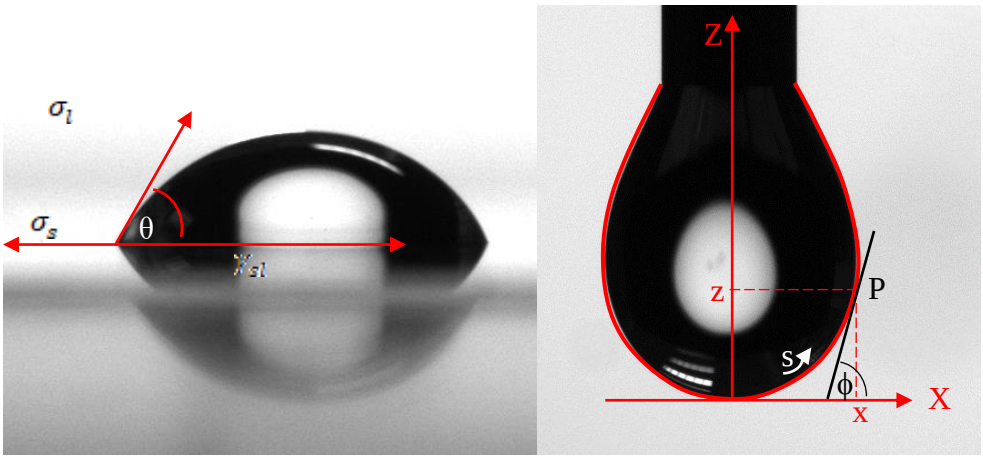

Figure 2.1. Visual of the drop shape analysis of (A) contact angle and (B) the surface tension pendant drop using the Kruss Easy Drop. The images are of the control solution (HNS+HNS) taken at 90 seconds. Figure is based off of figures appearing in the Kruss User's Manual (Kruss, 2010).

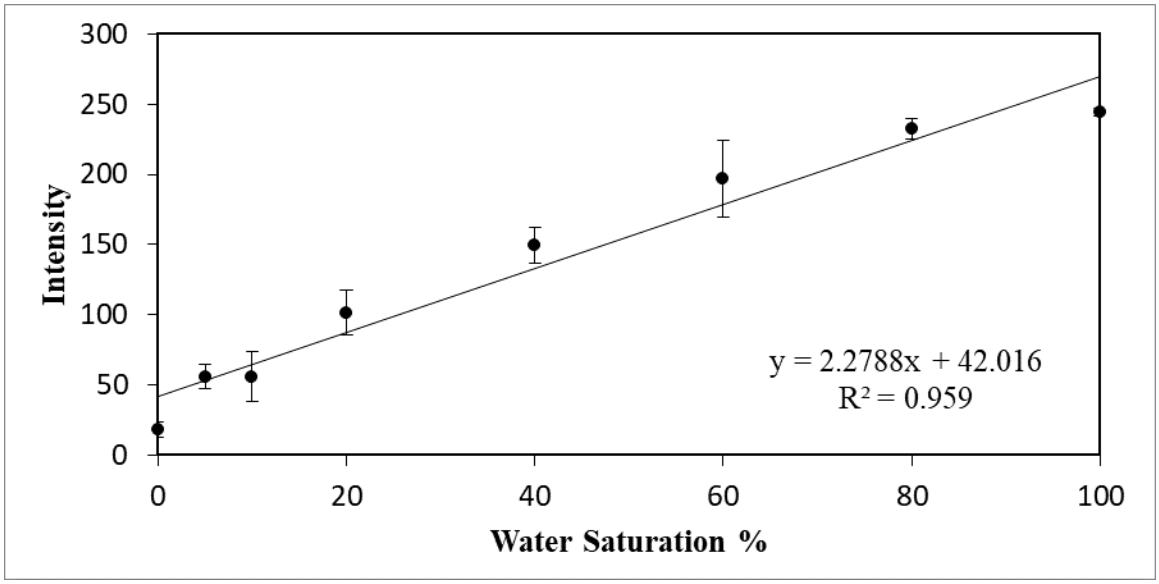

Figure 2.2. Empirical calibration curve with its linear trend line and slope equation. Intensity is a dimensionless value that may range from 0-255.

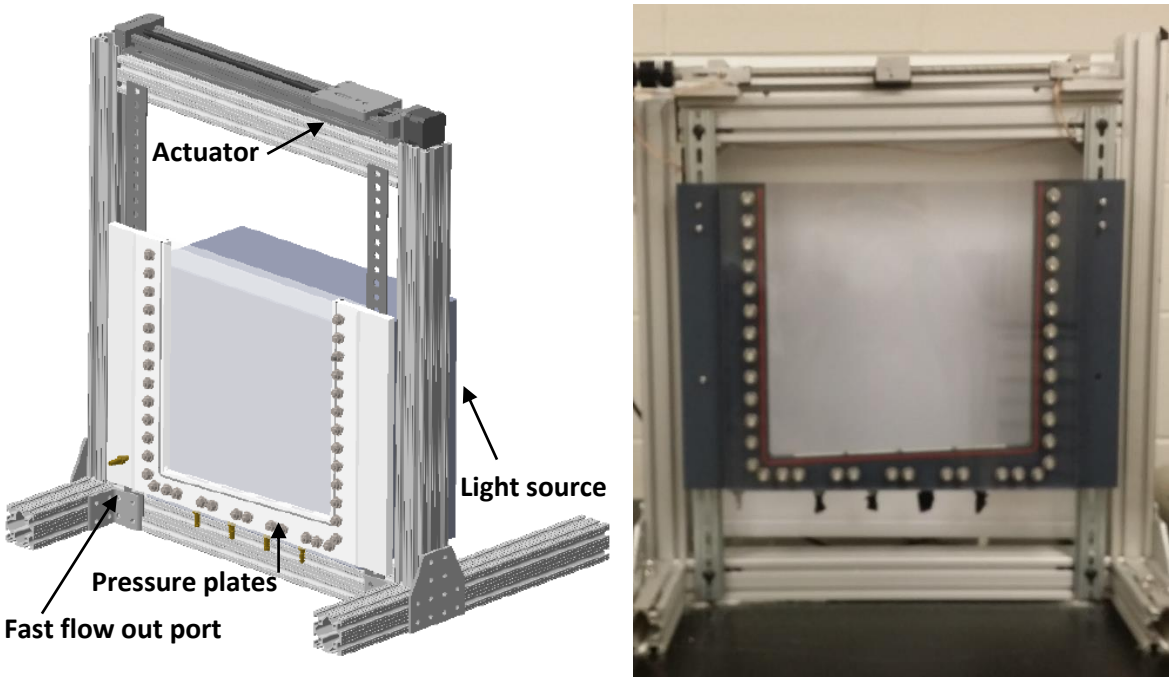

Figure 2.3. Experimental set up of the 2D tank system.

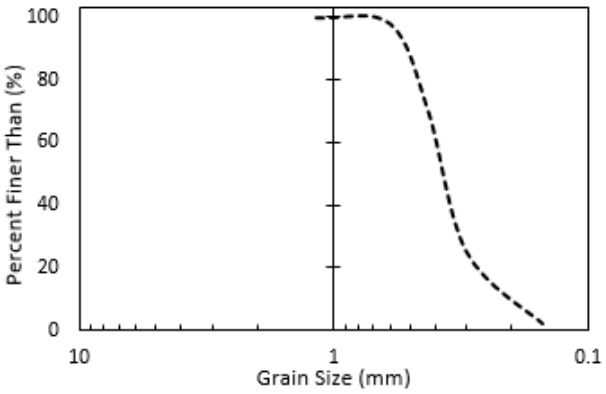

USA STND Sieve Mesh Size	Grain size (mm)	% of sand passing through (smaller than mm size)
16	1.18	100
30	0.6	98
40	0.425	70
50	0.3	25
100	0.15	2
pan (silts)		0

Figure 2.4. Characteristics and properties of the US Silica C778 ASTM graded sand.

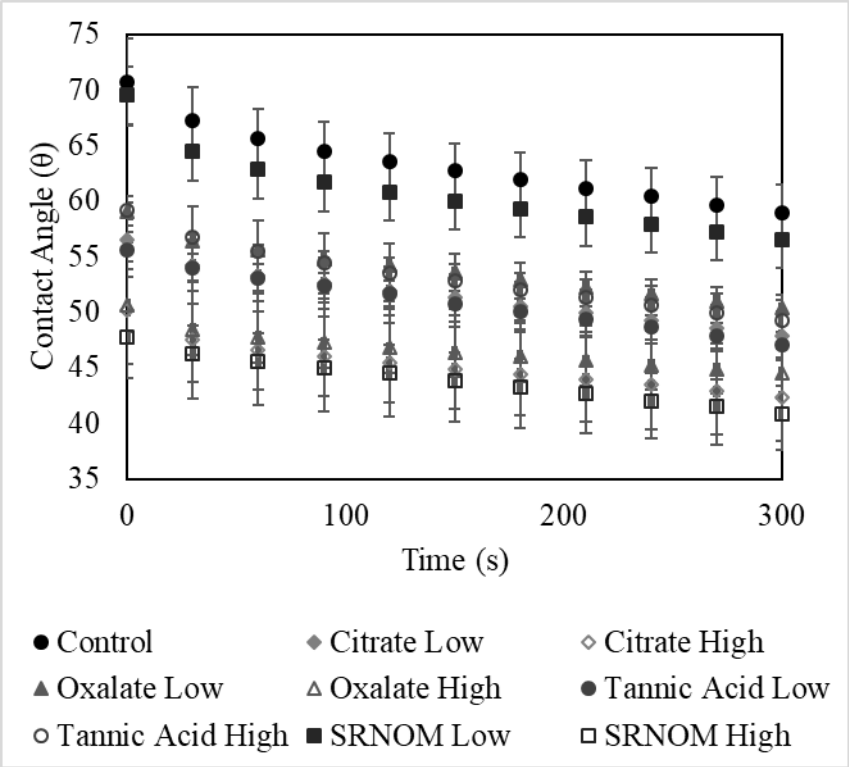

Figure 2.5. Dynamic contact angles of experimental solutions. Averages graphed, and associated error bars represent one standard deviation.

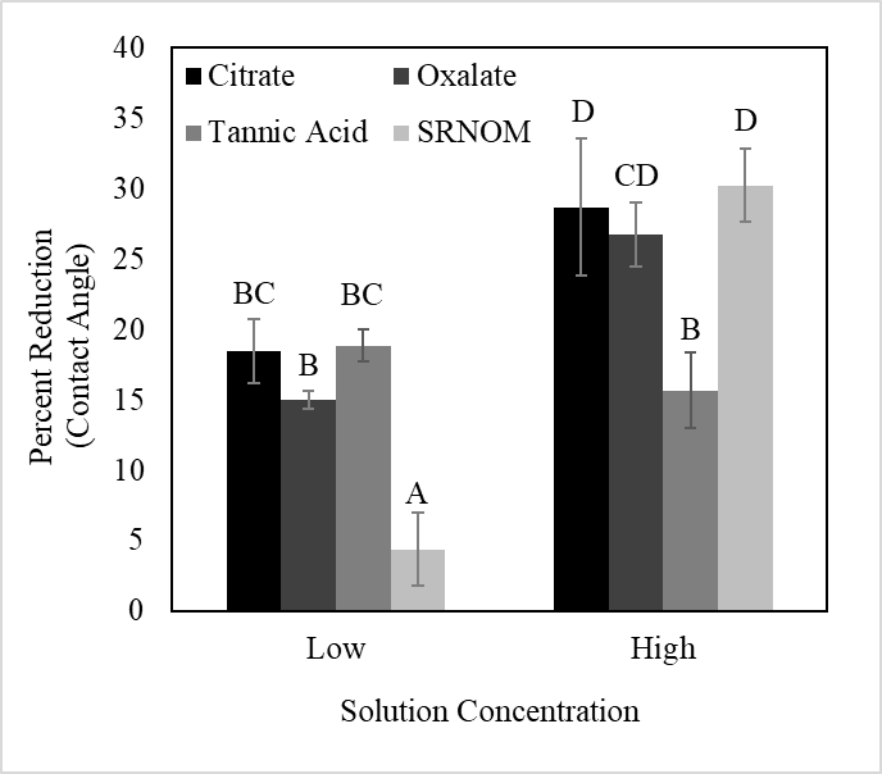

Figure 2.6. Percent reduction in contact angle from the control (group A), changes at stable time (90 seconds). Averages graphed and associated error bars represent one standard deviation.

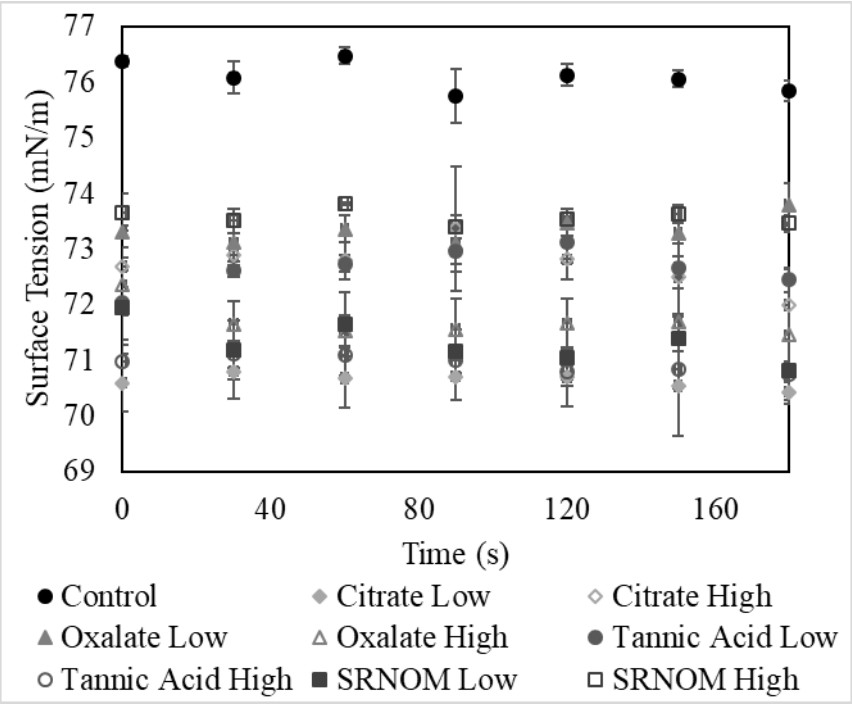

Figure 2.7. Dynamic surface tension of experimental solutions. Averages graphed, and associated error bars represent one standard deviation.

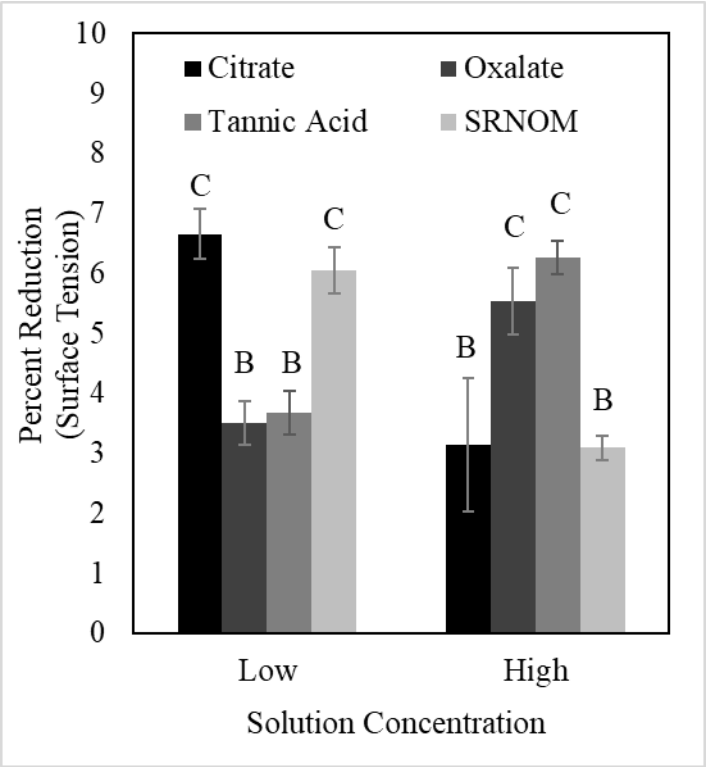

Figure 2.8. Percent reduction in surface tension from the control (group A), changes at stable time (90 seconds). Averages graphed and associated error bars represent one standard deviation.

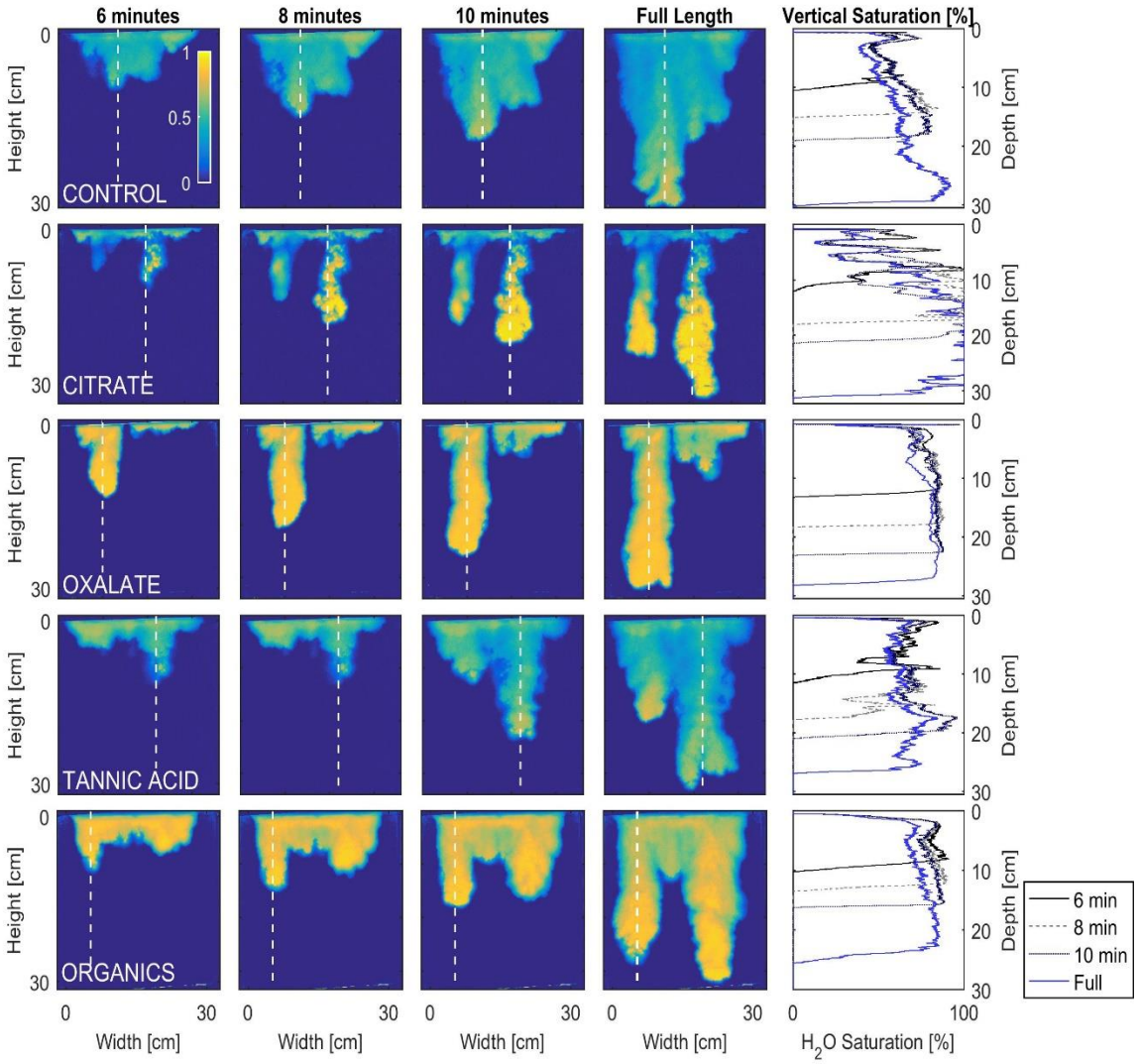

Figure 2.9. Multigraph comparison of the dynamic vertical profiles for low concentration exudates. The images are of the main finger over time.

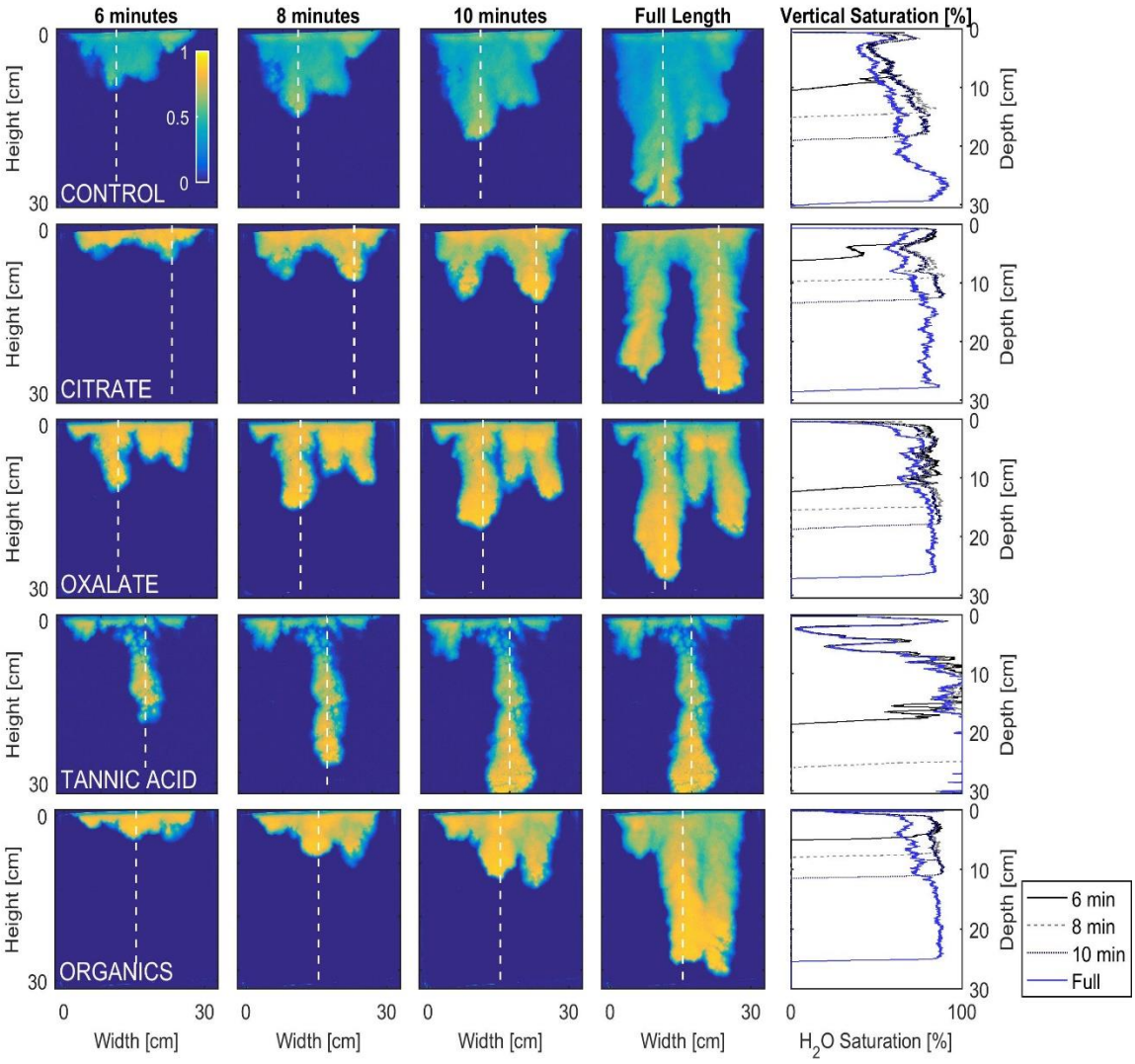

Figure 2.10. Multigraph comparison of the dynamic vertical profiles for high concentration exudates. The images are of the main finger over time.

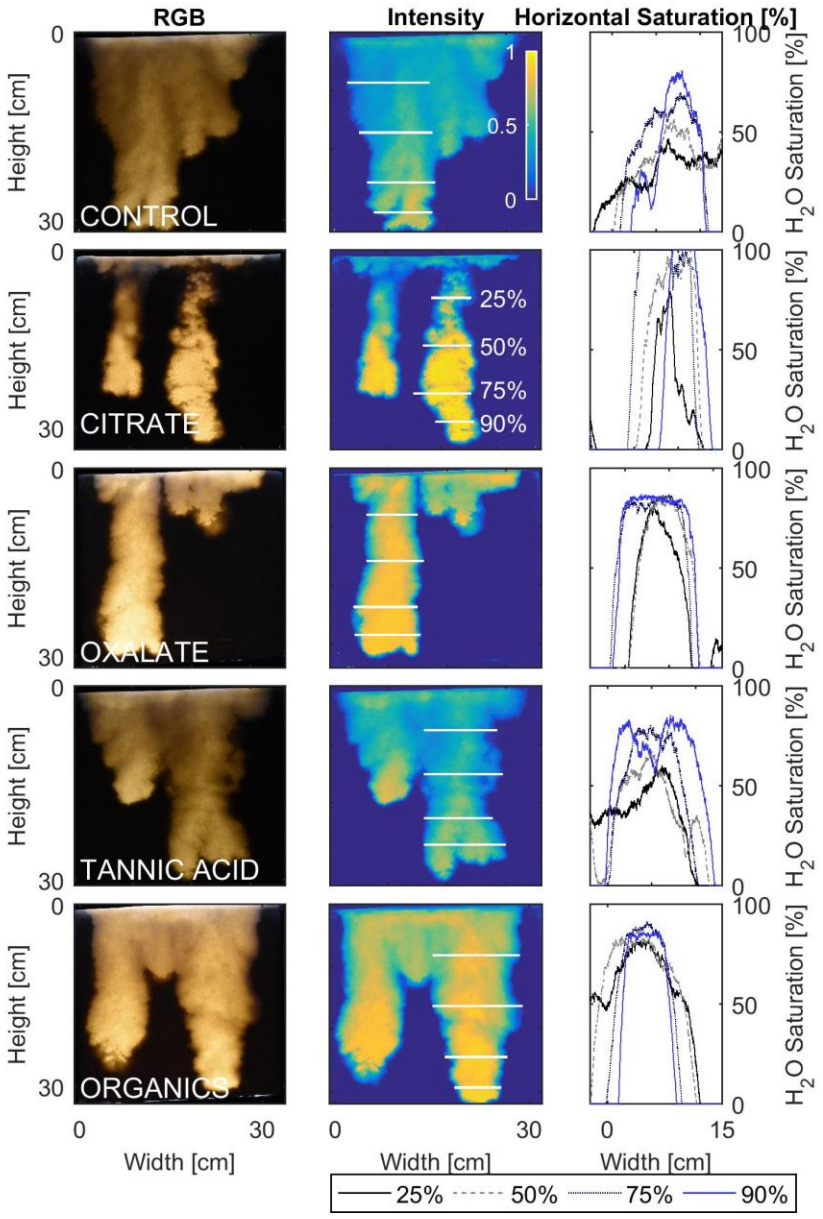

Figure 2.11. Multigraph comparison of the width profiles for low concentration exudates. The images are of the main finger at its full length. The location of the widths are measured at 25%, 50%, 75%, and 90% of the total fingers length.

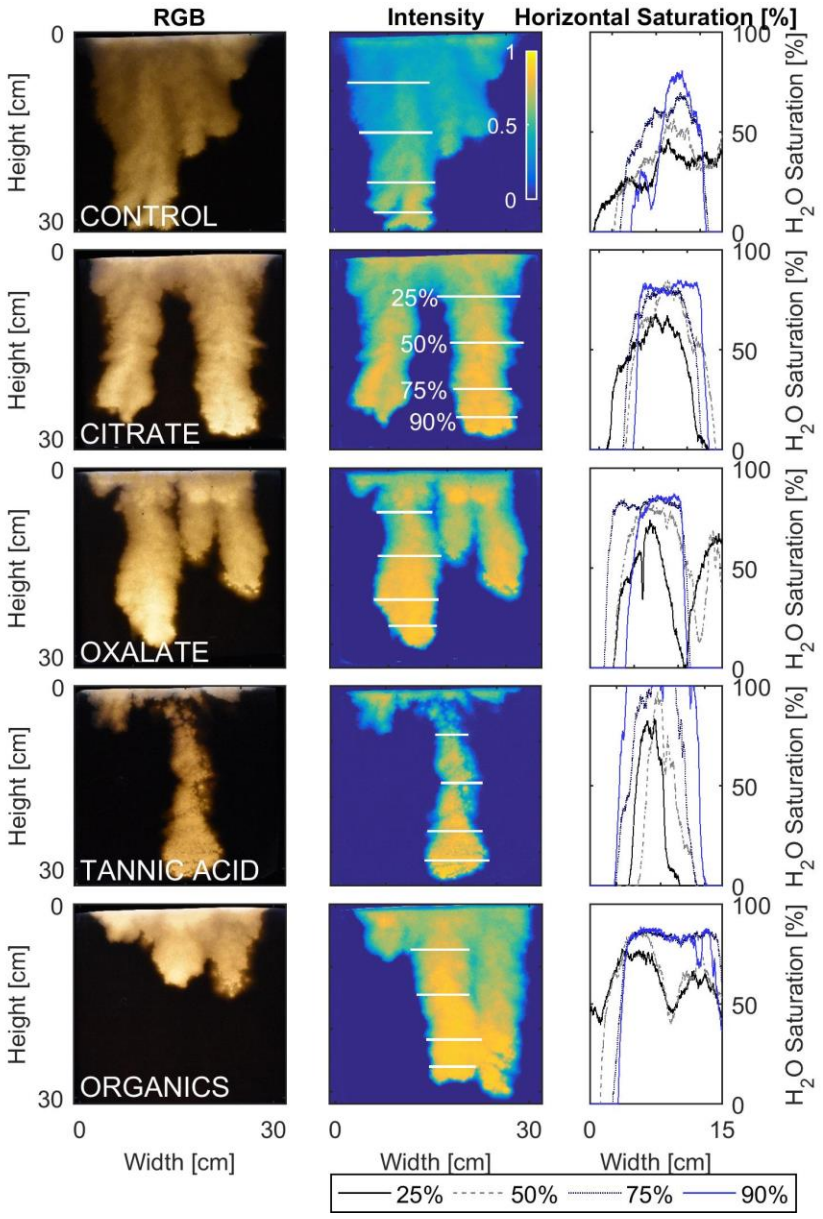

Figure 2.12. Multigraph comparison of width profiles for high concentration exudates. The images are of the main finger at its full length. The location of the widths are measured at 25%, 50%, 75%, and 90% of the total fingers length.

CHAPTER THREE

CONCLUSIONS

The effects of plant exudates on flow in the vadose zone have not been examined in detail (McCully,1999; Carminati et al., 2016; Zarebanadkouki et al., 2016). However, the effects of physical root impacts and mucilage impacts on soil hydraulic properties have been (McCully,1999; Carminati et al., 2016; Zarebanadkouki et al., 2016). Past work has shown that there are synergistic effects between exudates and mucilage on flow, but by understanding the variables separately we can better understand the whole system (McCully,1999; Walker et al., 2003). The objective of this research was to investigate the effects of plant root exudates on the infiltration processes through a porous media.

1. **Characterize the processes of the solid-liquid and liquid-gas interfaces of various biochemical compound solutions at a range of concentrations.**

The purpose of determining the interfacial characterization, through changes in the surface tension and contact angles, for each simulated exudate solution was to illustrate the significant changes occurring between the varying solutions and concentrations. The surface tension measurements were all significantly different from the control, though all the solutions displayed less than 10% reduction in the surface tension. The percent reduction in contact angle measurements displayed the greatest change from the control solution, except for the low concentration for SRNOM. Citrate at both the low and high concentrations displayed a large significant decrease in the contact

angle measurement, a 19% and 29% reduction accordingly. Oxalate was similarly significant, displaying a 15% and 27% reduction in contact angle for the low and high concentrations. Tannic acid at both concentrations displayed a 17% reduction, and the SRNOM was only significant at its highest concentration, a 30% reduction. These conclusions indicate that while unnaturally high concentrations of exudates do impact the interface properties, ultimately, significant changes are seen with normal concentrations. The implications of this understanding are that natural levels of exudates in the soil have a significant impact on flow through the rhizosphere.

2. Conduct 2D tank experiments with light transmission methodologies, to visualize and characterize infiltration processes.

Transient 2D flow experiments were conducted to compare and contrast how the physical application of the exudate solutions may differ from the interfacial characterization. It was found that the exudate systems for both concentrations did not display different finger geometries between the type or concentration of constituent, but did differ from the control system. Ultimately, the infiltration flow experiments behaved differently than would have been expected from the interfacial characterization conclusions. Ultimately, the 2D LTM tank experiments illustrated, that through our range of 0.1 – 500 mg/L solutions significant differences were seen in the interfacial characterization, ultimately the variations in our solutions were able to alter the flow systems from the control, but not between the various constituents. This conclusion is important, because of the range of complexity within the solutions tested; that a simple

molecule like citrate or oxalate, has relatively the same impact on the flow systems as a highly complex molecule like tannic acids.

REFERENCES

Carminati, A., Zarebanadkouki, M., Kroener, E., Ahmed, M. A., & Holz, M. (2016). Biophysical rhizosphere processes affecting root water uptake. Annals of Botany, 118, 561-571. doi: 10.1093/aob/mcw113

McCully, M. E. (1999). Roots in soil: Unearthing the complexities of roots and their rhizospheres. *Annu. Rev. Plant Physiol. Plant Mol. Biol*., 50, 695-718.

Walker, T.S., Bais, H.P., Grotewold, E., & Vivanco,J.M. (2003). Root exudation and rhizosphere biology. Plant Physiology, 132, 44-51. Doi:10.1104/pp.102.019661.

Zarebanadkouki, M., Carminati, A., & Ahmed, M. A. (2016). Hydrualic conductivity of the root-soil interface of lupin in sandy soil after drying and rewetting. Plant Soil, 398, 267-280. Doi:10.1007/s11104-015-2668-1.

APPENDICES

Appendix A

Secondary Tank Experimental Data Set

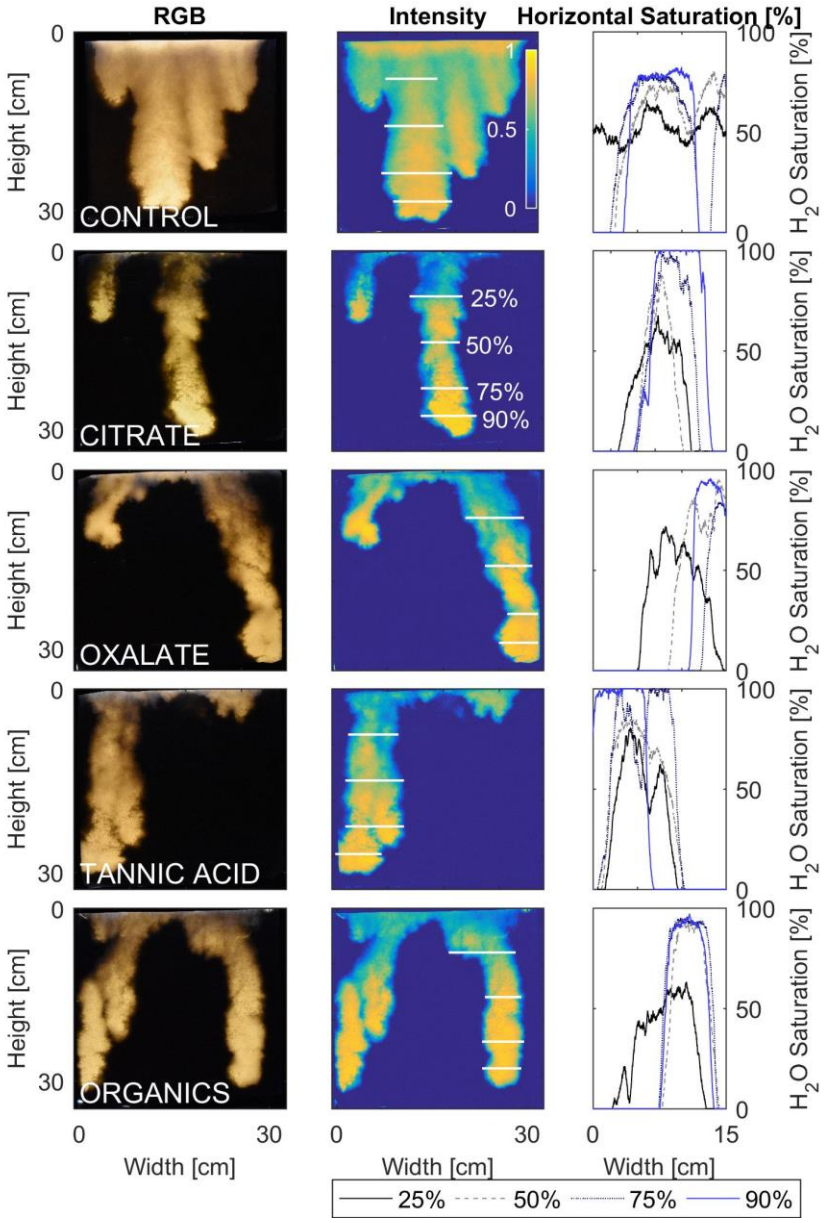

Figure 1A. Second tank experiment data set. Multigraph comparison of width profiles for high concentration exudates. The images are of the main finger at its full length. The location of the widths are measured at 25%, 50%, 75%, and 90% of the total fingers length.

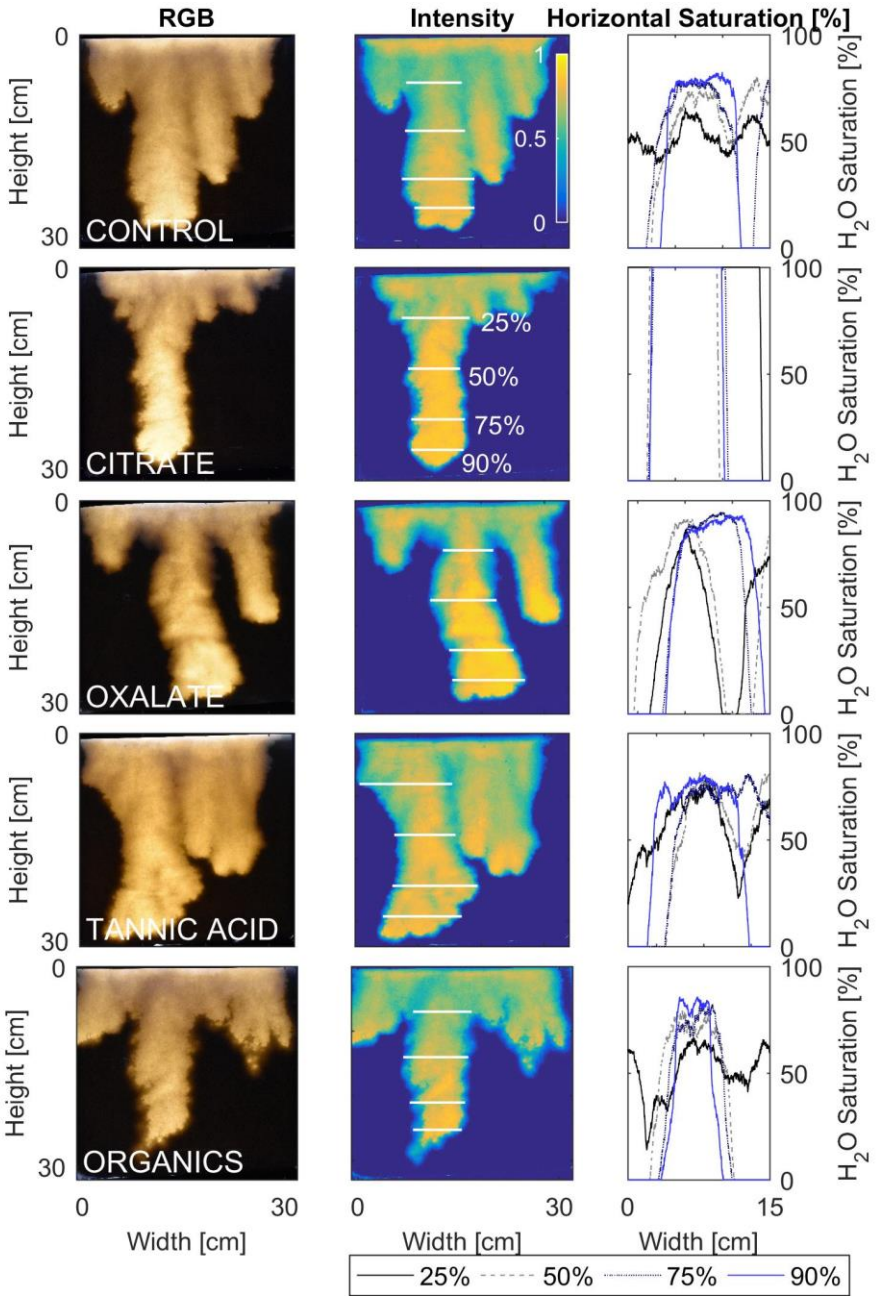

Figure 2A. Second tank experiment data set. Multigraph comparison of width profiles for low concentration exudates. The images are of the main finger at its full length. The location of the widths are measured at 25%, 50%, 75%, and 90% of the total fingers length.

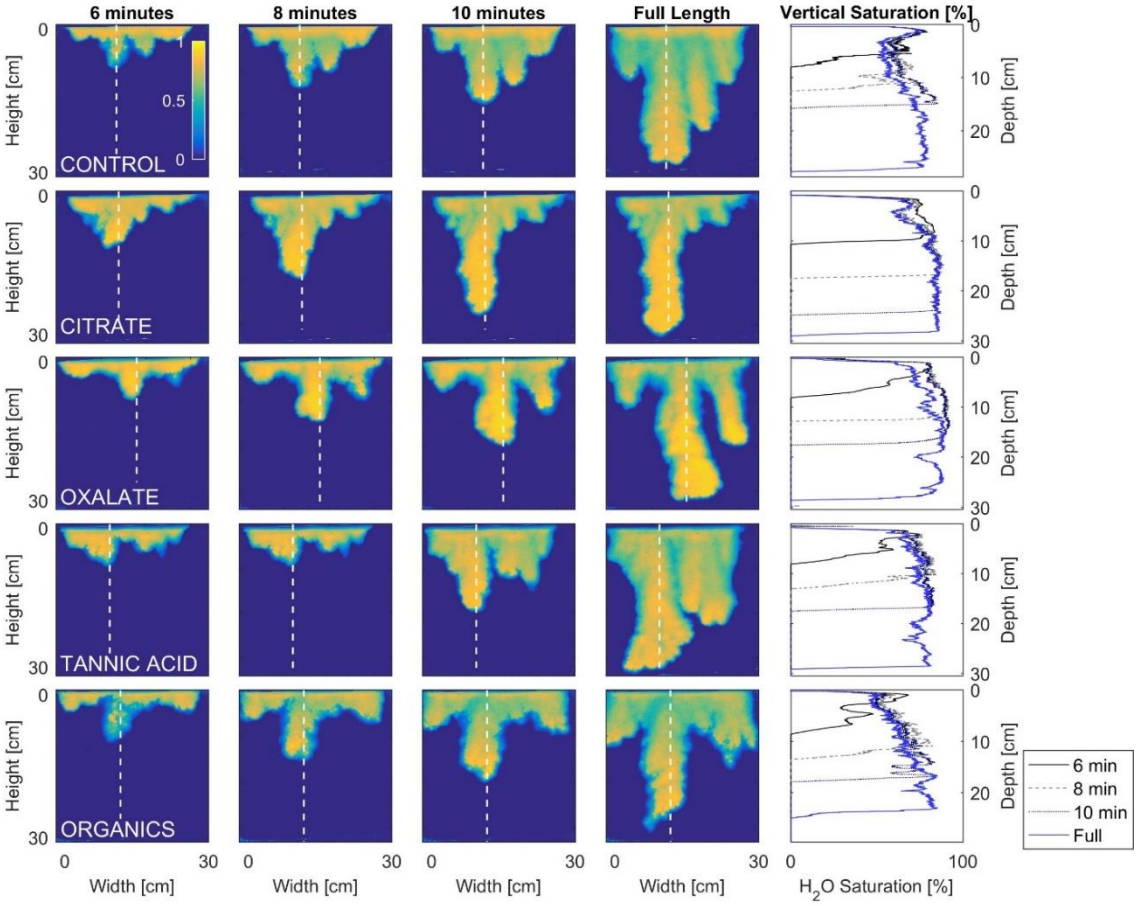

Figure 3A. Second tank experiment data set. Multigraph comparison of the dynamic vertical profiles for low concentration exudates. The images are of the main finger over time.

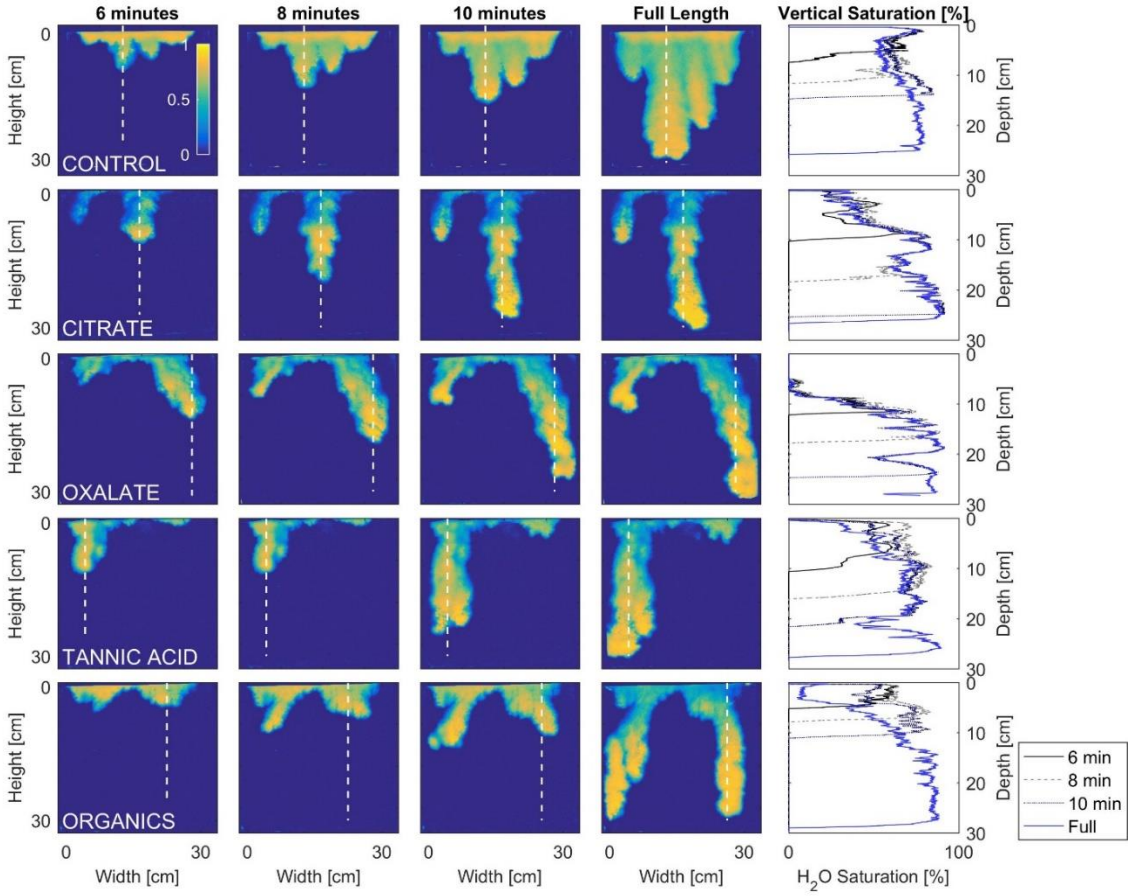

Figure 4A. Second tank experiment data set. Multigraph comparison of the dynamic vertical profiles for high concentration exudates. The images are of the main finger over time.

Appendix B

Standard Operating Procedures

PREPERATION OF THE HOAGLAND NUTRIENT AND EXUDATION SOLUTIONS

1.0 OBJECTIVE

The purpose of this protocol is to create the control and exudate solutions to be used in this work.

2.0 HEALTH AND SAFETY

Proper personal protective equipment such as, safety glasses, lab coat, and gloves must be worn at all times.

3.0 PERSONNEL/TRAINING/RESPONSIBILITIES

Any graduate research assistant familiar with the equipment and laboratory techniques and trained in this and references SOPs may perform this procedure.

4.0 MATERIALS

4.1 Supplies

1 L bottles
Weigh boats
De-ionized water
Sodium chloride
Sodium citrate
Sodium oxalate
Tannic acid
Suwanee River Natural Organic Matter
Nutrients needed for Hoagland Nutrient Recipe

4.2 Equipment

Scale

5.0 PROCEDURE

5.1 HOAGLAND NUTRIENT SOLUTION

A Hoagland Nutrient Solution (HNS) with 0.01 M NaCl (NaCl+HNS) was used as a control to simulate the requisite nutrients required of a plant to survive in a hydroponics system. The HNS was created by combining the components listed in Table 2.1 with 970 mL of ultrapure deionized (DI) water (18.2 MΩ•cm) with NaCl subsequently added to bring the solution to 0.01 M NaCl. These steps are based on the instruction of Arnon and Hogland (1940).

5.2 EXUDATE SOLUTIONS

The exudate solutions are created from the 0.01M NaCl plus Hoagland nutrient solution. The chemical exudate powders are weighed out according to table 2.2 and added to their respective solution containers.

INTERFACIAL CHARACTERIZATION: CONTACT ANGLE AND SURFACE TENSION

1.0 OBJECTIVE

The purpose of this protocol is to measure the solid-liquid (contact angle) and liquid-air (surface tension) interfacial characteristics of exudate solutions.

2.0 HEALTH AND SAFETY

Proper personal protective equipment such as, safety glasses, lab coat, and gloves must be worn at all times.

3.0 PERSONNEL/TRAINING/RESPONSIBILITIES

Any graduate research assistant familiar with the equipment and laboratory techniques and trained in this and references SOPs may perform this procedure.

4.0 MATERIALS

4.1 Solutions

0.01M NaCl and Hoagland Nutrient Solution
0.1 mg/L Sodium Citrate
500 mg/L Sodium Citrate
0.1 mg/L Sodium Oxalate
500 mg/L Sodium Oxalate
0.1 mg/L Tannic Acid
500 mg/L Tannic Acid
0.1 mg/L Suwannee River Natural Organic Matter
10 mg/L Suwannee River Natural Organic Matter

4.2 Supplies

100 mL beakers
De-ionized water
Disposable 1mL syringes
Reusable syringe needle tip
Silica glass cover slide

4.3 Equipment

Kruss Easy Drop DSA1 (FM40Mk2, Kruss GmbH, Germany)

5.0 PROCEDURE

5.1 Contact angle

Follow procedures outlined in the Kruss Drop Shape Analysis Manual, 8-13

5.2 Surface tension

Follow procedures outlined in the Kruss Drop Shape Analysis Manual, 14-17

TWO-DINEMSION TANK FLOW EXPERIMENTS WITH LIGHT TRANSMISSION METHOD

1.0 OBJECTIVE

The purpose of this procedure is to conduct simulated rain event infiltration flow systems in a 2D tank coupled with light transmission method to be able to quantify the water saturation profiles of various root exudate solutions.

2.0 HEALTH AND SAFETY

Proper personal protective equipment such as, safety glasses, lab coat, and gloves must be worn at all times.

3.0 PERSONNAL/TRAINING/RESPONSIBILITIES

Any graduate research assistant familiar with the equipment and laboratory techniques and trained in this and references SOPs may perform this procedure.

4.0 MATERIALS

4.1 Solutions

0.01M NaCl and Hoagland Nutrient Solution
0.1 mg/L Sodium Citrate
500 mg/L Sodium Citrate
0.1 mg/L Sodium Oxalate
500 mg/L Sodium Oxalate
0.1 mg/L Tannic Acid
500 mg/L Tannic Acid
0.1 mg/L Suwannee River Natural Organic Matter
10 mg/L Suwannee River Natural Organic Matter

4.2 Supplies

100mL beakers
500mL beakers
ASTM C778 graded US Silica sand
Electrical tape
Light-blocking cover (plastic)
Peristaltic pump tubing
Level
Flexible basin

4.3 Equipment

2D tank
Tank stand
Actuator and motor
Commercial LED light source
Sand packing device
Peristaltic pump
Nikon D5500 camera with standard 18-55mm lens
Camera tripod

5.0 PROCEDURES

5.1 Tank system set up

1. Place tank stand on a secure benchtop space
    a. Ensure LED light is securely attached to the stands back
    b. Ensure actuator rail system is affixed to the top of the stand
    c. Motor may be mounted onto stand as well or placed on the benchtop
    d. Place peristaltic pump next to stand set up on the benchtop
2. Screw the tank into place using the mounts on the front of the stand
    a. Make sure the tank is level

5.2 Sand loading

1. Attach sand packing device to the top of the tank opening
2. Place the flexible basin below the tank
3. Fill device with two tank volumes of sand
4. Quickly remove the barrier and allow sand to homogeneously fall
5. Remove the packing device and allow excess sand to fall into the basin
6. Gently tap the top of the tank to settle the top layer of sand
7. Brush off excess sand into basin

5.3 Flow experiments

1. Connect tubing through the pump and through to the actuator mount
    a. Leave enough slack for the actuator to move with the tubing
2. Place test solution in the 500mL beaker and place the tubing in it
3. Fix the light barrier around the tank and stand to ensure the only light seen is coming through the sand
    a. Check to make sure there are no bright spots where light is leaking through
4. Camera set up
    a. Use the cameras manual mode to ensure that the maximum intensity of any given pixel is less than 255.
    b. Using the time lapse feature an image is automatically taken every 30 seconds for the duration of the experiment
    c. Place the tripod at a distance from the tank set up to allow for full visualization of the tank
    d. Mark out the spot for future use
5. Turn off and block out all ambient light
6. Start the camera so that a background image is taken-0% saturated calibration
7. Start the pump after the first image has been taken
    a. Pump should dispense solution at a flow rate that does not exceed the saturated hydraulic conductivity of the porous media
8. Continue pumping until experiment is complete
    a. Allow the solution to pond at the bottom of the tank so the 100% saturation calibration is taken
9. Note the effluent volume

10. Break down, clean, repeat

5.4 Matlab analysis

1. Upload images to computer
2. Break the images apart into their respective hue, intensity, and saturation components
3. Find the linear calibration curve for the experiment
    a. 0%-100% saturation
4. Determine which is most applicable to your use (or combination of)
    a. Intensity used in this work
5. Use the calibration with the raw pixel information to find the saturation profiles
    a. Vertical saturation profiles
    b. Horizontal saturation profiles